University of Padua

Department of Engineering

Master's Degree Thesis in

BIOENGINEERING

Continuous glucose monitoring based algorithms for basal insulin therapy modulation in type 1 diabetes

Supervisor

Dr. Andrea Facchinetti

Co-supervisors

Prof. Giovanni Sparacino

Ing. Martina Vettoretti

Candidate

Lorenzo Meneghetti

Academic Year 2015/2016

A Giancarlo Osto,
mio nonno.

I would like to thank my supervisor, Ing. Andrea Facchinetti, for the patient guidance, motivation and advice he has provided throughout my work. I would also like to thank Prof. Giovanni Sparacino for the trust he put in me and Ing. Martina Vettoretti, who was very willing to assist me in each step to complete the thesis.
Thanks to my family for having always been supportive in every moment of my academic career. Thanks to my friends for all the good moments and laughs. A special thank to my grandmother, my number one supporter.

Abstract

The standard treatment for type 1 diabetes is based on exogenous insulin administrations tuned on the sparse blood glucose (BG) measurements. Recently, this standard therapy has been improved by the introduction of continuous glucose monitoring (CGM) sensors, which allows measuring in a quasi continuous way BG concentration for several days, and insulin pumps for the subcutaneous insulin infusion.
In the last few years, thanks to the availability of such "continuous" data streams, particular attention has been paid to the development of strategies for the real-time modulation of the basal insulin therapy to prevent, or at least mitigate, risky hypoglycemic episodes by exploiting CGM data stream information. In particular, most relevant strategies for basal insulin modulation are based on the "static risk" (SR) concept, which is logarithmic transformation of BG measurements into a risk values, fed with either the actual BG value or the predicted ahead-of-time BG value obtained using a simple linear predictor (LP). In addition, these algorithms have been developed and tested on unrealistic simulated scenarios.
The aim of the present thesis was to develop a realistic in-silico framework to study, starting from the Univ. of Padova/Univ. of Virginia type 1 diabetes simulator, to test the performance of literature insulin algorithms for the basal insulin therapy modulation and to present new methodologies for such a scope. First, a new in-silico scenario was implemented which allows to generate realistic hypoglycemic episodes that could happen after a meal. Then, state-of-art algorithms for basal insulin modulation were modified by first substituting the SR with the "dynamic risk" (DR) concept, which improves SR by integrating in the formulation also the information on the glucose trend, and second by replacing the simple LP algorithm for the real-time prediction of glucose concentration with a more sophisticated autoregressive model (AR) with forgetting factor.
Results obtained on 100 virtual subjects created with the modified Univ. of Padova/Univ. of Virginia type 1 diabetes simulator shows that the use of DR in place of SR in the basal insulin modulation strategy improves the number of prevented hypoglycemic cases and lowers the average time-spent in hypoglycemia, and that the performance are even better when the proposed AR prediction algorithm is also used.

Contents

Chapter 1

Glucose sensors and their use in insulin therapy of type 1 diabetes

1.1 Diabetes mellitus

The term ”diabetes mellitus”, commonly referred to as diabetes, describes a metabolic disease of multiple etiology characterized by chronic elevated levels of blood glucose (BG) or hyperglycemia with disturbances of carbohydrate, fat and protein metabolism resulting from defects in insulin secretion, insulin action, or both [1]. Diabetes is a chronic disorder of metabolism that afflicts about 347 million people in the world and this number is estimated to grow in the following years.
There are several pathogenetic processes that are involved in the development of diabetes:

- **Type 1 diabetes (T1D)** In type 1 diabetes, the hyperglycemia condition is caused by an absolute deficiency in insulin production caused by autoimmune destruction of the beta cells of the pancreas, with the presence of certain antibodies in blood. It usually develops in children and adolescents although it can also occur later in life. Patients affected with T1D require lifelong insulin injections for survival. Insulin injections can be administered with different combinations: short-acting/long-acting, intensive management with multiple injections prior to meals, once or twice daily injections, insulin pumps.

- **Type 2 diabetes**
  Type 2 diabetes is characterized by a hyperglycemia due to a defect in insulin secretion usually with a contribution from insulin resistance condition. It usually develops during adulthood although is on the rise in children and adolescents. Type 2 diabetes is usually but not always associated with obesity, decreased physical activity and unhealthy diets

and involves insulin resistance in nearly all cases. Patients do not require lifelong insulin treatment but can control blood glucose with diet and exercise alone, or in combination with oral medications, or with the addition of insulin.

In the short term, diabetes causes symptoms of increased thirst (polydipsia), increased urination (polyuria), increased hunger (polyphagia) and unexplained weight loss. Over time, it can cause cardiovascular disease[5], foot ulcers[6], retinopathy[7], kidney failure[8] and death[9].
In this thesis we will focus particularly on hypoglycemia prevention in T1D because it represents one of most feared symptoms and one of the major causes of mortality.

1.2 Blood glucose monitoring: SMBG and CGM

Apart from symptoms relief, diabetes treatment strategy is mainly focused on targeting normal blood glucose levels (70-180 mg/dL) during the day. In order to do so patients are required to regularly inject insulin doses on the basis of the glycemia measured in the blood. To this purpose they are equipped with glucometers to self-measure blood glucose and receive education about self-monitoring for sign/symptoms of hypoglycemia and hyperglycemia. Currently, the standard technique through which health providers and patients assess the effectiveness of the management plan is the finger-stick self-monitoring of blood glucose (SMBG).

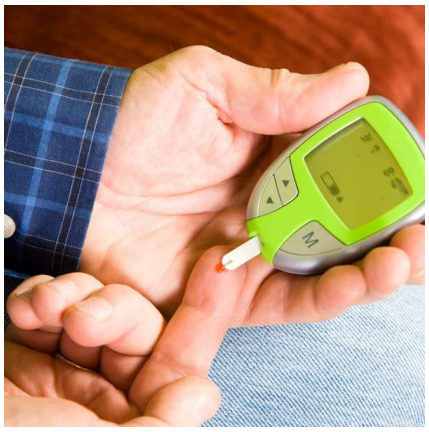

Fig. 1.1: SMBG finger stick procedure: a finger is pricked with a lancet to obtain a small quantity of capillary blood for testing (taken from [10]).

It is based on the use of lancet devices as shown in figure 1.1: the patient pricks his finger to obtain a small quantity of capillary blood that can be analyzed to reveal its current blood glucose value. These measures should be performed prior to meals and snacks, occasionally post-prandially, at bedtime, before exercise and when low blood glucose is suspected [11].

Unfortunately, in addition to worsening a patient's quality of life by requiring multiple actions per day, the few measurements performed with a SMBG device do not provide a complete description of glucose trend during the day. Continuous glucose monitoring (CGM) was proposed 15 years ago and represents a more promising technology for diabetes control, as we can see in figure 1.2.

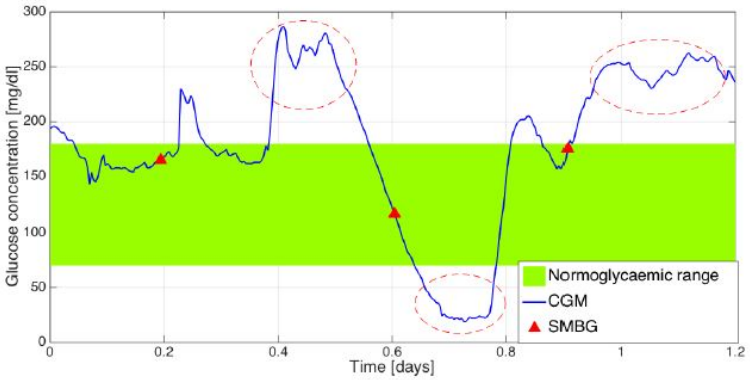

Fig. 1.2: Comparisons between SMBG and CGM measurements derived info for diabetes treatment

A continuous glucose monitor (CGM) typically consists of a sensor, a wireless transmitter, and a receiver that allows the user to follow his interstitial glucose values throughout the day. Some receivers can also be integrated with a sensor-augmented insulin pump (see section 1.3). The sensor consists of a wire inserted subcutaneously most commonly into the abdomen, that measures interstitial glucose via generation of an electrical current when glucose reacts with the enzyme glucose oxidase. The receiver provides the user a 24-h continuous display of glucose data, collected every 5-10 min. Glucose values are displayed on a receiver, insulin pump display, or smartphone. In figure 1.3 an example of a CGM sensor (Dexcom G4) is shown.

Fig. 1.3: Abdomen inserted CGM sensor (taken from [14]).

CGM provides not only discrete glucose values, but also the benefit of the glucose history including trends, rate of glucose change as well as the direction of the change.
In clinical research, continuous glucose monitoring, with nearly continued use, was associated with reduced time spent in hypoglycemia and a concomitant decrease in HbA1c in children and adults with type 1 diabetes. [12]. Results in children have been more disappointing, although clearly increased use in the older (but not the younger) children is related to their efficacy. The use of these devices does not lead to improved quality of life outcomes, although satisfaction with the devices has been consistently strong in both adults and children. [13]
From the practical point of view, it is interesting noting that the Food and Drug Administration (FDA) did not allow CGM system labels to include nonadjunctive use that is their direct usage for making therapy adjustments without the indication of a finger stick, because of concerns of inaccuracy that could lead to inappropriate treatment decisions. Past CGM systems, including the Dexcom G4, Medtronic Enlite, and FreeStyle Navigator, received regulatory approval in the United States specifically for adjunctive use, with labeling indicating treatment decisions are to be based on blood glucose values obtained through SMBG, not CGM readings. CGM systems are already being used for diabetes treatment decisions in Europe. The Abbott Navigator II is approved for use in determining insulin doses when glucose is not changing. Most recently, the Dexcom G5 Mobile CGM system is now approved in Europe to be used nonadjunctively [15].
Along with the above described benefits CGMs come with another interesting feature that is their usage in combination with automated insulin pumps.

1.3 Insulin pumps

An insulin pump is a machine which enables insulin to be delivered either automatically, or in response to instructions given by the pump wearer. It drip feeds insulin into the body through the day and can also deliver larger doses of insulin whenever needed, such as before meals. Insulin pumps can be connected to the body via tubing or attached to the surface of the skin with a patch and controlled remotely.
In figure 1.4 we can see an example of a tethered insulin pump: a small tube (cannula) goes into and just under the skin and is held in place by an adhesive patch. It allows insulin to pass from the tubing into the body. The display screen displays information to the wearer that are chosen interactively trough buttons. The motor turns round and causes the plunger to push insulin through the reservoir and into the tubing as visualized in figure 1.5.
Insulin pumps use only quick acting insulin and deliver two different types of dose: bolus and basal. The bolus is the dose of insulin that is specifically

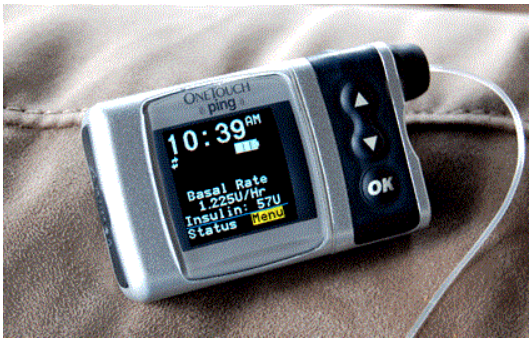

Fig. 1.4: OneTouch Ping insulin pump (taken from): [16])

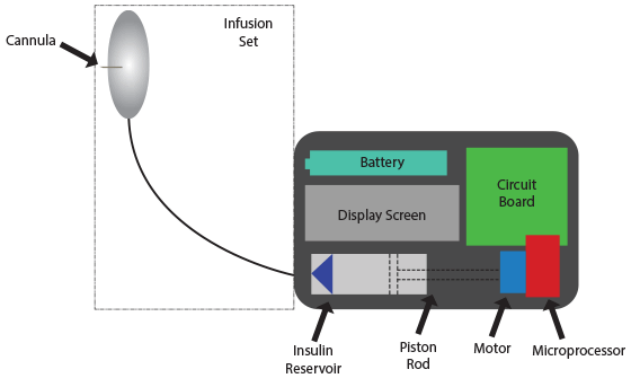

Fig. 1.5: Automated insulin pump diagram (taken from: [17])

taken at meal times to help control blood glucose levels following a meal. This dose mimics the insulin peaks evoked by the pancreas response that occur in non-diabetic people. The basal dose represents a background dose of insulin that is delivered constantly during the day, the same way as a non-diabetic person pancreas would do. Basal insulin keep blood glucose levels steady during periods of fasting. Figure 1.6 shows an example of insulin infusion during the day, including basal insulin delivery and meal insulin boluses.

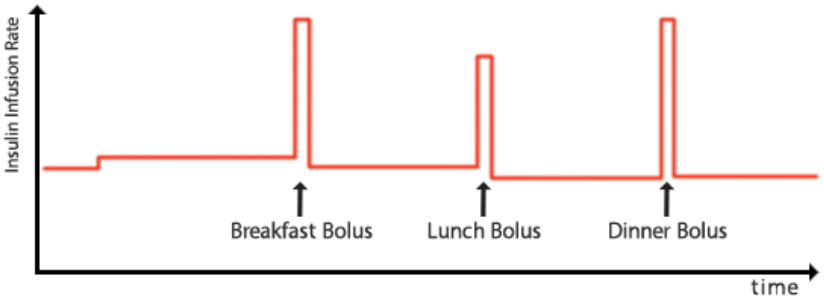

Fig. 1.6: Insulin delivery scheme during the day (taken from: [18])

Most pumps on the market can be set to deliver different rate of basal insulin

for each hour of the day as planned with the physician. This can be a great benefit since the need for background insulin can be variable at different parts of the day.
UK National Institute for Health and Care Excellence reviewed different group studies of adults and childred of mixed age and found that insulin pump therapy resulted in improvement of HbA1c results and a reduced incidence of severe hypoglycemia cases [19]. Insulin pumps give more control of blood glucose levels over night and so they can help to reduce the chances of having overnight hypoglycemic episodes, one of the main causes of mortality in young patients affected with type 1 diabetes. [20]

1.3.1 CGM augmented insulin pumps

The most modern trend in insulin pump technology is for pumps to directly interact with CGMs. Pumps that allow CGM integration include: Medtronic MiniMed 640G, Medtronic MiniMed Paradigm Veo, Animas Vibe with Dexcom G4 sensors. Animas vibe pump possess an on board food database to help with carb counting. This pump is also a strong choice for people that are specifically looking for a pump integrated with the Dexcom G4 Platinum, which is, at time of writing, the most accurate CGM available (according to diabetes.co.uk). The MiniMed 640G and Paradigm Veo can suspend insulin if the sensor falls below a threshold and the user does not respond to an alarm. [21]
The possibility of integrating a predictive algorithm to modulate basal insulin delivery and prevent hypoglycemic episodes has been object of intensive study lately. The following chapter will give an overview of some of the studies on this matter.

Chapter 2

CGM-based modulation of insulin therapy

2.1 Modulation of insulin injection

Hypoglycemic episodes can be prevented by pre-emptively acting on the ampunt of insulin that is injected into the organism. Since the quantity introduced with the boluses cannot be reduced once in the circulation, many studies explored the possibility of modulating the injection of basal insulin. In the present chapter we will review three popular approaches. The first is due to Buckingham et al. who evaluated the pump suspension feature that is a pump shut-off for a given amount of time in response to a predicted hypoglycemia event based on current BG. The second methodology was proposed by Hughes et al., who defined their method, consisting of insulin gradual attenuation depending on a risk function, calculated basing on true or predicted hypoglycemia values using a predictive Kalman filter. A third methodology was presented by Patek et al. as part of a three-layer modular architecture for the control of diabetes and is based on a linear predictor and a modulation based on a risk function similar to the one described by Hughes et al.

2.2 Pump suspension approach

Different articles were published by Buckingham et al. to evaluate the feasibility of preventing hypoglycemic episodes by insulin pump suspension triggered by a predicted glucose value. A first study 2.2.1 on a small group of patients evaluated the performances of two predictive algorithms while second study 2.2.2 involved a system of different algorithms working simultaneously. Extended randomized clinical trials were also performed to evaluate the pump suspension feature overnight.

2.2.1 First clinical study

In 2009 Buckingham et al. [22] analyzed the performance of two different prediction algorithms in an experiment of induced hypoglycemia in 21 T1D patients. Alongside they evaluated the duration of basal insulin hypoglycemic effect. Glycemia monitoring was performed using the FreeStyle NavigatorÂő (Abbott Diabetes Care, Alameda, CA). One algorithm was a modification of the Navigator alarm, which uses a short-term linear extrapolation and uncertainty threshold to predict hypoglycemia. The second algorithm was developed at Stanford and is based on multiple empirical, statistical models that are used to estimate future glucose values. An increase in the prediction horizon produce a bigger amount (60-80%) of prevented cases of hypoglycemia in this scenario. The analysis of the duration of basal insulin hypoglycemic effect resulted in the following: after 30 mins rate of change was maintained, after 75 mins it reached zero. Following 90 mins of pump suspension, no hyperglycemia episodes (BG level $>$ 180 mg/dL) were observed.

2.2.2 Algorithm combination approach

Dassau et al. in 2010 [23] tested a hypoglycemia prediction algorithm (HPA) using data from past clinical admissions in patients with mean age of 20 years. The system involved the use of 5 different algorithms working simultaneously to predict hypoglycemic situations with adjustable prediction horizon (35, 45, 55 mins). When a quorum amount (1-5) of algorithms produced a glycemic predicted value above a defined threshold (70, 80, 90) an insulin pump-shutoff was requested for 90 mins.

The algorithms used in the system are described here shortly.

Linear prediction: the linear projection (LP) uses the past 15 minutes glucose values to obtain a linear extrapolation. The angular coefficient of the straight line obtained is then considered as hypothetic glycemia trend and used to project the future values.

Kalman filtering (KF): a Kalman filter is used to estimate glucose and its rate of change, which are then used to make predictions about future glucose levels. The filter is tuned to trade off the probability that a measured glucose change is real versus the result of sensor noise.

$$\underbrace{\begin{bmatrix} g_{k+1} \\ d_{k+1} \\ f_{k+1} \end{bmatrix}}_{x_{k+1}} = \underbrace{\begin{bmatrix} 1 & 1 & 0 \\ 0 & 1 & 1 \\ 0 & 0 & 1 \end{bmatrix}}_{\Phi} \underbrace{\begin{bmatrix} g_k \\ d_k \\ f_k \end{bmatrix}}_{x_k} + \underbrace{\begin{bmatrix} 0 \\ 0 \\ 1 \end{bmatrix}}_{\Gamma^W} w_k$$

$$y_k = \underbrace{\begin{bmatrix}1 & 0 & 0\end{bmatrix}}_{\mathrm{C}} \underbrace{\begin{bmatrix}g_k \\ d_k \\ f_k\end{bmatrix}}_{x_k} + v_k$$

The states are: blood glucose concentration (g_k), its rate of change (d_k), the rate of change of the rate of change (f_k).
$\hat{x}$ is estimated then

$$\hat{x}_{k|k-1} = \Phi \hat{x}_{k-1|k-1}$$

once y_k is available

$$\hat{x}_{k|k} = \hat{x}_{k|k-1} + L(y_k - C\hat{x}_{k|k-1})$$

L_k is the steady-state Kalman gain matrix.
The Kalman gain L is calculated using the covariances Q and R. Given that these covariances are not known in advance, they become tuning parameters. Changing the relative weight between Q and R serves to trade off the confidence in the model versus the confidence in the measurement.
The approach is presented in more details in simulation studies by Palerm et al. [27]

Hybrid infinite impulse response:
A linear discrete-time-signal-processing method [24] generates output predictions using previous output (glucose measurements) without input (insulin infusion). The filter coefficients are used together with the predicted outputs for a prediction horizon and are updated when prediction and parameter error are larger than user-specified bounds. The filter performances can be tuned by adjusting window length, prediction horizon and error criteria.

Statistical prediction: a probability of hypoglycemia is generated and thresholded using multiple empirical, statistical models [25] to estimate future blood glucose. The prediction algorithm is divided into three components:
1) calibration, which converts raw CGM and capillary blood glucose measurements into a physiologically consistent, accurate blood glucose history;
2) prediction, which uses training data and the recent calibrated blood glucose history to generate predictions and associated accuracy estimates;
3) hypoglycemic alarming, which transforms the predictions and accuracy estimates into a probability of the patient becoming hypoglycemic, which is then thresholded into a binary alarm.

Numerical logical algorithm: a three-point calculated rate of change using backward difference approximation and the current glucose value are used into logical expressions to detect impending hypoglycemia.

$$f'(x_{i+1}) \approx \frac{3y_{i+1} - 4y_i + y_{i-1}}{x_{i+1} - x_{i-1}}$$

The logical expressions verify that:
- the rate of change is both negative and within an acceptable range
- the CGM glucose values are within predefined boundaries and that a pending hypoglycemic event is predicted within the threshold time window

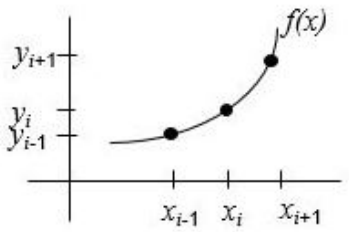

Fig. 2.1: Three point backward difference

Numerical logical algorithm provides insensitivity to sensor signal dropouts and easy tuning.

Hypoglycemia was defined for glucose readings < 60 mg/dL by the Freestyle Navigator. The best results (91% of hypoglycemic events predicted) were obtained when setting the prediction horizon to 35 min, the voting threshold to three of five algorithms and a glucose threshold of 80 mg/dL. With a four of five algorithms requirement, 82% of the events were predicted. The authors highlighted the fact that balance between aggressiveness of the HPA and effectiveness is an important factor since too many false alarms are a detriment to safety systems and will result in disconnecting of the system by the user, rendering the system useless.
Buckingham et al [26] published a followup article, where they evaluated the algorithm performances on clinical trials. They observed a mean difference of 12 mins between the second and the third algorithm activation. The difference between the FreeStyle Navigator system and the true glucose values at the time of pump suspension was 4±9 mg/dl (mean±SD) for successful events, 18±10 mg/dl when the predictive pump shutoff failed. The reasons why CGMs were consistently reading higher blood glucose values in unsuccessful prediction events were attributed to CGM inaccuracy or known lag time between the two compartments.

2.2.3 Randomized clinical trials

Another study from Buckingham group in 2003 [28] performed randomized clinical trials on 19 participants (18-56 years old) with type 1 diabetes. They used a pump suspension system communicating with a laptop computer containing the prediction algorithm which was a Kalman filter-based model. The laptop contained a randomization schedule that indicated whether the algorithm would be in operation that night (intervention night) or would not be activated (control night). Audible glycemic alarms were produced at 60 mg/dL and 250 mg/dL. Different prediction horizon were tested (30, 50, 70 min), with the addition of different pump suspension criteria. The results showed that the algorithm appeared to be successful in reducing nocturnal hypoglycemia ($\leq$ 70 mg/dL) by 40%. The number of nights with prolonged

hypoglycemia ≤60 mg/dL for more than 1 h was reduced by 60%. Overall, they demonstrated that pump suspension is safe and feasible with use of a bedside computer communicating with an insulin pump and CGM device.
In 2015, a more recent clinical study [29] involved a 42 nights (each) trial with children with T1D (11-14 and 4-10 years). Important results in the cumulative time >120/180 min in hypoglycemia although there was still not total prevention.
Pump suspension feature was evaluated with different studies [30] [31] [32] to assess the fact that it can be used as a mean to reduce the risk of nocturnal hypoglycemia.

2.3 The brakes/power brakes approach

In their study presented in 2009 [33], Hughes at al., presented 2 algorithms:

- Brakes: based on continuous glucose monitoring data
- Power brakes: based on continuous glucose monitoring data and insulin pump data

Both algorithms implemented a red/yellow/green light alert system, to inform the user on the risk of hypoglycemia.

2.3.1 Brakes

The brakes algorithm macro scheme can be visualized in figure 2.2

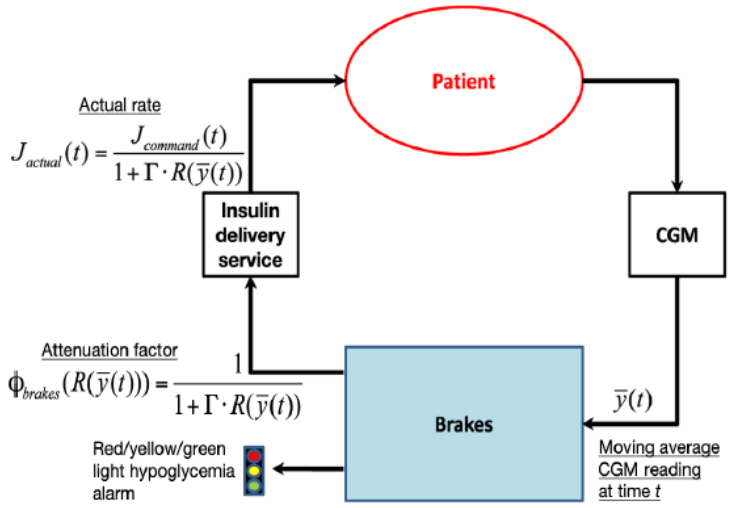

Fig. 2.2: Brakes algorithm scheme (taken from [33])

The BG value of the patient is read by the CGM and is then used by the brakes algorithm to modulate the rate of basal insulin that would be normally delivered. A "traffic light" alarm is also generated to alert the patient of a possible predicted hypoglycemic episode. The attenuation factor Φ_{brakes} is computed after assessing a patient's current risk $R(\bar{y}(t))$ of hypoglycemia:

$$\Phi_{brakes}(R(\bar{y}(t))) = \frac{1}{1 + \Gamma \cdot R(\bar{y}(t))} \tag{2.1}$$

where $\Gamma = e^{-0.7672-0.0091 \cdot TDI+0.0449 \cdot CF}$ is the "aggressiveness parameter" and $\bar{y}(t)$ represents the patient's current BG state and is calculated as the 15 min non-weighted moving average of CGM reading

$$\bar{y}(t)\frac{1}{15}\sum_{i=0}^{14} CGM(t-i) \tag{2.2}$$

The algorithm modifies the current rate of insulin $J_{command}$ that would be administered by the pump without brakes, utilizing the calculated attenuation factor:

$$J_{actual}(t) = \Phi_{brakes}(R(\bar{y}(t)))J_{command} \tag{2.3}$$

The risk function is calculated as follows:

$$R(\bar{y}(t)) = \begin{cases} 10[\alpha(ln(\bar{y}(t))^{\beta} - \gamma)]^2 & \text{if } 20 < \bar{y}(t) < 120 \text{ and } \dfrac{d\bar{y}}{dt} < 0 \\ 100 & \text{if } \bar{y}(t) \leq 120 \\ 0 & \text{otherwise} \end{cases} \tag{2.4}$$

Where $\alpha = 0.918642$, $\beta = 1.29286$ and $\gamma = 7.57332$.

2.3.2 Power brakes

In the power brakes algorithm (figure 2.3) insulin injected information is used in conjuction with glucose values as we can see in figure. Insulin delivery rate is calculated accounting for the insulin that has been injected in the past.

The risk of hypoglycemia $R_m(\bar{y}(k))$ is now derived from a metabolic state observer, using a compartmental "minimal model" [34].

$$x(k+1) = Ax(k) + Bu(k) + G\omega(k) \tag{2.5}$$

where $x(k)$ is the state of the system at sample time k, $u(k) = J_{actual}(k) - J_{basal}(k)$ (J_{basal} being the minimum value over the patient's basal rate profile) is the insulin input at stage k and $\omega(k) = meal(k) - meal_{ref}(k)$ is the ingested glucose disturbance signal at stage k. The state observer is based on a steady state kalman filter, based on knowledge of $u(k)$ and y(k)

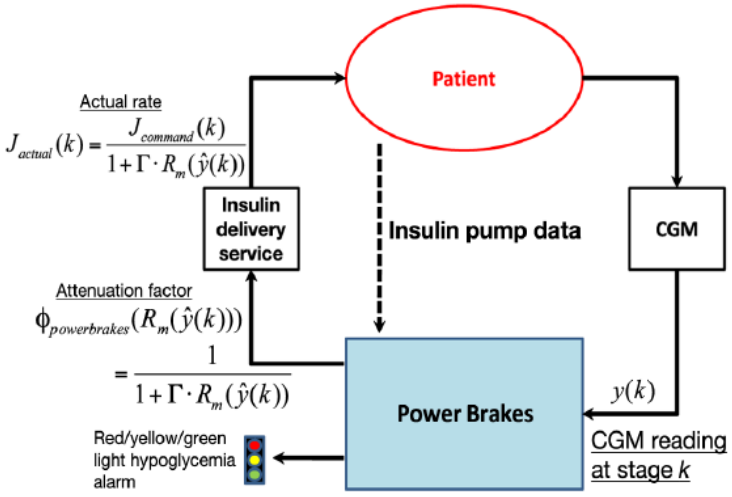

Fig. 2.3: Power brakes algorithm scheme (taken from [33])

$$y(k) = CGM(k) - G_{ref} \tag{2.6}$$

Where CGM(k) is the readout of the continuous glucose monitor at k and G_{ref} is a glucose reference value (here set at 112.5 mg/dl).
The measurement signal is modeled as:

$$\hat{y}(k) = Cx_\tau(k) \tag{2.7}$$

where $C^T = \begin{bmatrix} 1 & 0 & 0 & 0 & 0 & 0 & 0 & 0 \end{bmatrix}$ and $x_\tau(k)$ is the metabolic state observer.
The metabolic state is expressed recursively:

$$\hat{x}(k|k-1) = A\hat{x}(k|k-1) + Bu(k-1) \tag{2.8}$$

$$\hat{x}(k|k) = \hat{x}(k|k-1) + L_f(y(k)) - C\hat{x}(k|k-1) \tag{2.9}$$

where

$$L_f = AP_fC^T(CP_fC^T + R_S)^{-1} \tag{2.10}$$

and P_f is the unique stabilizing solution to the algebraic Riccati equation

$$A^TPA - A^TPG(G^TPG + R_S)^{-1}G^TPA + Q_S = P \tag{2.11}$$

Therefore the projected BG concentration at stage k is computed as follow

$$\hat{y}(k) = C\hat{x}_\tau(k) \tag{2.12}$$

where τ represents an amount of time corresponding to the length of the prediction window.

$$\hat{x}_\tau(k) = A^\tau \cdot \hat{x}(k) + A_\tau B \cdot u(k) + A_\tau G \cdot w(k) \tag{2.13}$$

$$A_\tau = \begin{cases} 0 & \text{if } \tau = 0 \\ \sum_{s=0}^{\tau-1} A^\tau & \text{if } \tau > 0 \end{cases} \tag{2.14}$$

When τ is set to 0 the risk is based only on the best estimate of BG given all the data received up to stage k, when $\tau > 0$ an assessment of the future risk of hypoglycemia is performed, τ minutes ahead. Finally the prediction is used to calculate the attenuation factor, using a modified version of the brakes formula

$$J_{actual}(t) = \Phi_{powerbrakes}(R(\hat{y}(t)))J_{command}$$

$$\Phi_{powerbrakes}(R_m(\hat{y}(t))) = \frac{1}{1 + \Gamma \cdot R_m(\hat{y}(t))} \tag{2.15}$$

$$R_m(\hat{y}(t)) = \begin{cases} 10[\alpha(ln(\hat{y}(t))^\beta - \gamma)]^2 & \text{if } 20 < \hat{y}(t) < 120 \text{ and } \dfrac{d\hat{y}}{dt} < 0 \\ 100 & \text{if } \hat{y}(t) \leq 120 \\ 0 & \text{otherwise} \end{cases} \tag{2.16}$$

Where $\alpha = 0.918642$, $\beta = 1.29286$ and $\gamma = 7.57332$.
The green/yellow/red traffic light signal system was design to alert the user as to their level of hypoglycemic risk. It worked as follows:
In brakes,

- if $R(\bar{y(t)}) = 0$, the green light is triggered
- if $R(\bar{y(t)}) > 0$ and $\bar{y(t)} \leq K_{red}$, the yellow light is triggered
- if $R(\bar{y(t)}) < K_{red}$, the red light is triggered K_{red} is chosen as 80 mg/dL.

In power brakes,

- if $Rm(\hat{y}(t)) = 0$, the green light is triggered
- if $Rm(\hat{y}(t)) > 0$ and $\bar{y}(t)_{shutoff}(t) \geq K_{red,IOB}$, the yellow light is triggered
- if $Rm(\hat{y}(t)) < K_{red}$, the red light is triggered

2.3.3 In silico testing results

The efficiency of the algorithms were evaluated using the FDA-accepted University of Virginia/University of Padova Metabolic Simulator at the University of Virginia. Two scenarios designed to cause hypoglycemia were taken into consideration, an highly variable insulin sensitivity and a skipped meal. To simulate the first one, a doubled rate of basal insulin was delivered to all 100 adult patients of the simulator, all of them starting from a BG concentration of 150 mg/dL. To simulate the second one a premeal bolus was delivered, avoiding the corresponding meal. The amount of this premeal bolus was designed such that the subject will drop to a BG concentration of 50 mg/dl.
The percentage of hypoglycemia predicted events using Brakes and Power Brakes was of 80% and 94% respectively for the first scenario and 83% and 93% for the second scenario.

2.4 Brakes approach exploiting linear prediction

In their study published in 2012, Patek et al. [35] introduced a three-layer modular architecture for the control of diabetes, consisting in a sensor/pump interface module (IM), a continuous safety module (CSM), and a real-time control module (RTCM), which separates the functions of insulin recommendation (postmeal insulin for mitigating hyperglycemia) and safety (prevention of hypoglycemia). A section of the CSM, the safety supervision model (SSM), was designed to continuously monitor the patient's state and to authorize insulin recommendations intervening when needed to prevent hypoglycemia.

2.4.1 Linear prediction algorithm

Based on the history of CGM samples received up to the current time the data coordination and state estimation blocks of the SSM compute a BG estimate $\hat{G}(k)$ (mg/dL) for the current control update cycle k. The estimate is computed as:

$$\hat{G}(k) = \bar{G}(k) + 17 \cdot \dot{G}(k) \tag{2.17}$$

where $\bar{G}(k)$ (mg/dL) is the unweighted average of CGM samples received in $(t-10, t]$ and $\dot{G}(k)$ (mg/dL/min) is the slope of the least-squares linear fit of all CGM samples received in $(t-30, t]$.
The attenuation of basal insulin factor is calculated in similar fashion to the one proposed by Hughes et al:

$$\phi(\rho(k)) = \frac{1}{1+\rho(k)} \tag{2.18}$$

The risk function $\rho(k)$ is adapted from the BG symmetrization function introduced in [36] and is computed as follows:

$$\rho(k) = \begin{cases} 0 & \breve{G}(k) \geq 112.5 \\ 10[a(ln((\breve{G}(k))^b - c)]^2 & \breve{G}(k) \in (20, 112.5) \\ 100 & \breve{G}(k) \leq 20 \end{cases} \tag{2.19}$$

where a = 1.509, b = 1.084, and c = 5.381, and

$$\breve{G}(k) = 0.5 \cdot (G^*(k) + \hat{G}(k)) \tag{2.20}$$

$G^*(k)$ is the estimated BG corrected through interactions with other modules: the modulation algorithm that takes into account information from the delivery history of insulin up to the current time and assess the current amount of insulin on board (IOB) Ic(k) and uses this to estimate $G^*(k)$ that reflects the impact of correction IOB through

$$G^*(k) = \hat{G}(k)[\hat{I}_c(k)]^+ \cdot \theta_{corr}(k) \tag{2.21}$$

Insulin on board related calculations are not reported here, please refer to [35] for details. The algorithm was presented as part of a modular architecture for closed-loop control of diabetes therefore the algorithm performances were not isolatedly evaluated.

2.5 Aim of the thesis

As we have seen in this chapter, basal insulin modulation algorithms seem to be a powerful tool to avoid hypolgycemia, especially in an open-loop setup. Therefore it is important to develop an in-silico simulation environment to evaluate the efficacy and the performances of these algorithms. The aim of this thesis will be to implement inside the Padova/UVA Type 1 diabetes metabolic simulator (see section 4.2.1) a module that allows to simulate real-time functioning of algorithms for basal insulin modulation therapy. In particular we will reimplement the following literature algorithms:

- the Brakes insulin attenuation algorithm (see section 2.3.1) based on "Static Risk" (SR), function presented in Hughes et al. [33]
- the linear prediction (LP) algorithm (see section 2.4) as described in Patek et al. [35] limited to the BG estimation performed without the corrections through the interactions with the other modules of the three-layer architecture.

  Therefore:

$$\phi_{LP}(\rho(k)_{LP}) = \frac{1}{1 + \rho_{LP}(k)} \tag{2.22}$$

and

$$\rho_{LP}(k) = \begin{cases} 0 & \hat{G}(k) \geq 112.5 \\ 10[a(ln((\hat{G}(k))^b - c)]^2 & \hat{G}(k) \in (20, 112.5) \\ 100 & \hat{G}(k) \leq 20 \end{cases} \quad (2.23)$$

are calculated using $\hat{G}(k)$ from equation 2.17, to compute, with reference to equation 2.3,

$$J_{actual}(t) = \phi_{LP}(\rho_{LP}(k))J_{command} \quad (2.24)$$

The two previous algorithms for basal insulin modulation are based on simple assumptions and/or algorithms. In particular, the Brakes SR formula performs a simple transformation of the current glucose value which does not take into account its trend. This means, as we will see later in chapter 3, that equal glucose values produce the same risk value despite of their predicted behaviour (e.g approaching hypoglycemic threshold of moving away from it). The brakes approach by linear prediction is based on a simple prediction algorithm that may not be effective in all situations, being the algorithm a simple linear extrapolation of the current glucose value and trend. Therefore in the next chapter we will also try to evaluate the possible improvements on the algorithm performance by:

- replacing the SR formula with the "dinamic risk" (DR), a risk function of glucose concentration introduced by Guerra et al. [37] which calculates the glucose risk on the basis of glucose value and its trend.
- replacing the LP described in Patek et al. [35] with a autoregressive (AR) model based prediction introduced by Sparacino et al. [38].

Chapter 3

Improvements of the algorithms for CGM-based modulation of basal insulin

3.1 Use of the dynamic risk

3.1.1 The dynamic risk concept

A previous study by Kovatchev et al. [36] already suggested that the glycemic range is asymmetric. The hypoglycemia range is much narrower than the hyperglycemic range and health threats increase faster when moving deeper in the first versus the latter range.
Let us consider for example glucose levels of 40 mg/dL or 210 mg/dL: even if the two levels stay at an equal absolute distance from the hypo/hyperglycemic threshold (70 and 180 mg/dL) the first condition corresponds to sever hypoglycemia while the second one to mild hyperglycemia. It is obvious now that the risk for the patient increases much faster when glucose trend is moving below the hypoglycemic threshold compared to when it moves above the hyperglycemic threshold.
Figure 3.1 displays a simulated continuous glucose profile. Points A1, A2, B1 and B2 are highlighted and labeled together with a portion of the tangent line to the glucose profile in these points. Circle labeled as C represents a particular event of hypoglycemic threshold crossing. Both A1 and A2 represent a glucose concentration just below the hypoglycemic threshold but with different derivatives, whereas B1 and B2 represent two episodes of hypoglycemic threshold crossing again with two different derivatives. Using this example is now clear that if only we were to use SMBG measurements to define the patient risk when in one of those 4 points we would not have a complete information. In fact the clinical risk associated with A1 is far more dangerous than the one with A2 because in the first case the patient is heading deeper in the hypoglycemia region while in the other one he is recovering. Similarly B2

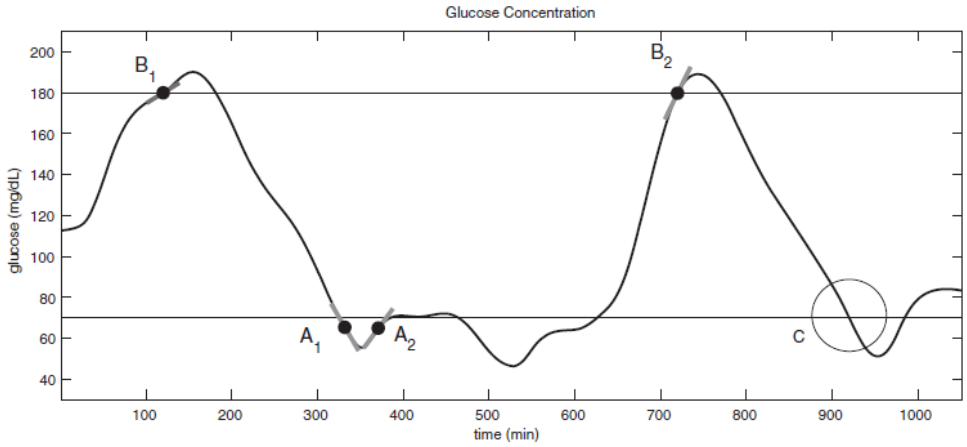

Fig. 3.1: Simulated glucose profile: equal glycemic values (A1 and A2 or B1 and B2) may not represent a situation of equivalent health risk

situation is more dangerous than B1 because the patient is going faster into the hyperglycemic region.
The original methodology proposed by Kovatchev et al. [36] calculates the standard risk (SR) function $r(g)$ given a generic glycemic level g

$$r(g) = 10 \cdot f(g)^2 \tag{3.1}$$

where

$$f(g) = \gamma \cdot [(ln(g))^\alpha - \beta] \tag{3.2}$$

With α, β and γ being scalars equal to 1.084, 5.381 and 1.509. The above function $r(g)$ maps the glycemic range (20-600) mg/dL to the (static) risk space range (0-100).
Starting from $r(g)$, two quantities, the low and high glucose risk, $r_l(g)$ and $r_h(g)$, respectively, are defined as

$$R_l(g) = \begin{cases} r(g) & \text{if } f(g) < 0 \\ 0 & \text{otherwise} \end{cases} \tag{3.3}$$

$$R_h(g) = \begin{cases} r(g) & \text{if } f(g) > 0 \\ 0 & \text{otherwise} \end{cases} \tag{3.4}$$

To distinguish the risk coming from situation A1 versus A2 and B1 versus B2 for example a modification in the risk calculation is required. A DR measure has to be defined that takes into account not only the glycemic value but also the derivative of its trend. Conceptually this requires a function in the form of:

$$DR = \Phi(g, \frac{dg}{dt}) \tag{3.5}$$

DR function should be able to have two desirable properties:

1. in stationary conditions (derivative = 0)

$$DR(g, 0) = r(g) \tag{3.6}$$

   that is when glucose value is stable DR should equal SR.

2. when glucose is moving toward critical hypo/hyperglycemic regions, $r(g)$ should be amplified whereas it should be attenuated when g is approaching normoglycemia.

The solution proposed is:

$$DR(g, \frac{dg}{dt}) = \begin{cases} SR(g) \cdot e^{+\mu \frac{dr}{dt}} & \text{if } SR(g) > 0 \\ SR(g) \cdot e^{+\mu \frac{dr}{dt}} & \text{if } SR(g) > 0 \end{cases} \tag{3.7}$$

where r is the function of g of equation 3.1.
The following equation

$$\frac{dr}{dt} = \frac{dr}{dg}\frac{dg}{dt} = \{10\gamma^2 \cdot [(ln(g))^{2\alpha-1} - \beta(ln(g))^{\alpha-1}] \cdot 2\alpha\frac{1}{g}\} \cdot \frac{dg}{dt}$$

can be exploited to obtain a calculation of $\frac{dr}{dt}$, with α, β and γ equal to those defined before. Figure 3.1 displays the effect of dynamic risk compared to simple risk.

3.1.2 Use for basal insulin modulation

In this thesis we will test the effect of the replacement the standard risk formula that is calculated in the brakes algorithm with a dynamic risk.
Specifically, with reference to equation 2.1, we will substitute $R(\bar{y}(t))$ with $DR(\bar{y}(t))$ that is calculated with:

$$DR(\bar{y}(t)) = \begin{cases} DR(g, \frac{dg}{dt}) & \text{if } 20 < \bar{y}(t) < 120 \\ 100 & \text{if } \bar{y}(t) \leq 120 \\ 0 & \text{otherwise} \end{cases} \tag{3.8}$$

where $DR(g, \frac{dg}{dt})$ is calculated as in 3.7, and proceed on calculating the attenuation factor as:

$$\Phi_{brakes}(DR(\bar{y}(t))) = \frac{1}{1 + \Gamma \cdot DR(\bar{y}(t))} \tag{3.9}$$

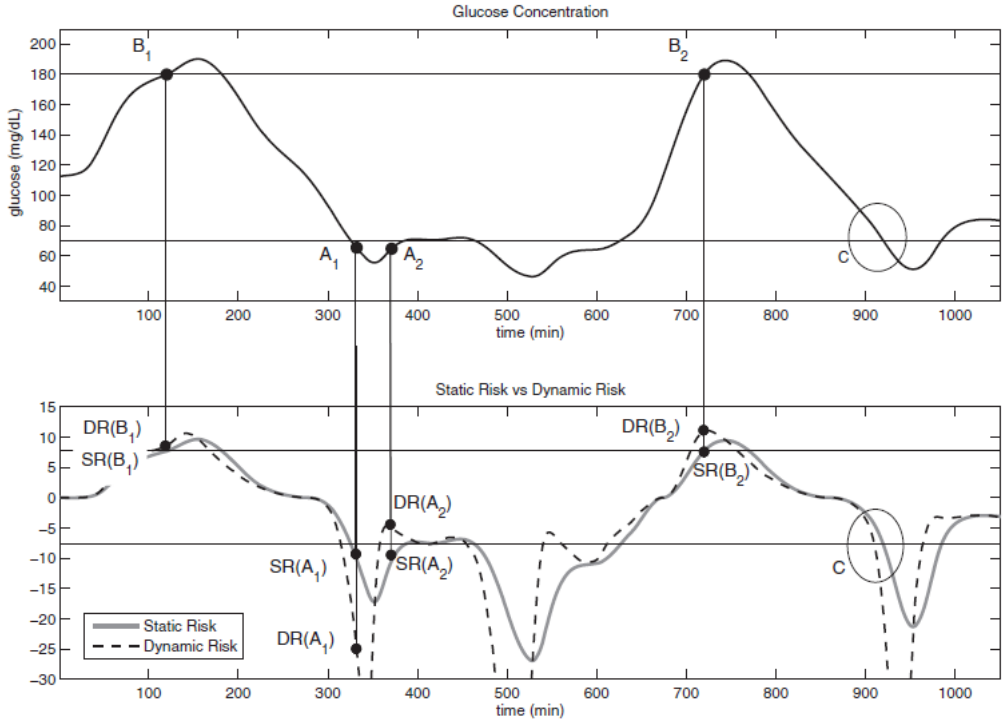

Fig. 3.2: Comparison between Static risk (above) and Dynamic risk (below): risk is amplified when moving towards the hyper/hypoglycemic zone.

3.2 AR model based prediction

Hypo/hyperalerts can be generated on the basis of ahead-of-time prediction of glucose concentration by using past CGM data and suitable time-series models. In their paper, Sparacino et al. [38] evaluated the possibility of describing past glucose data by a first-order autoregressive (AR) model. Following a time-varying modeling approach: at each sampling time, a new set of model parameters is first identified by means of weighted least squares techniques. Then, the model is used to forecast glucose level for a given prediction horizon (PH).
Considering a generic auto-regressive (AR) model structure:

$$y(n) = a_1 * y(n-1) + a_2 * y(n-2) + ... + a_p * y(n-p) + w(n)$$

Where $y(n)$ represents the glucose sample at time t(n), $w(n)$ is a random variable with variance σ^2, $a_1...a_p$ are the model variables. The set of parameters $\theta = [\sigma^2, a_1, ..., a_p]$ is estimated using Linear Least Squares weighted with forgetting factor (μ). Once Θ is determined, the model is used to calculate the prediction of glucose level T steps ahead, i.e., $\hat{\Theta}_{n+T}$.
The way with which past data are weighted is a key aspect in model fitting. Here, the weight μ^k is assigned to the sample taken k instants before the actual sampling time, i.e., is the weight of the sample at time t_{n-k}. The parameter

behaves like a forgetting factor. The forgetting factor μ, thus, belongs to the range (0,1) and its value regulates the length of the "memory" of the past data which participate to the determination of theta.
The algorithm can be summed up with the following equations:

$$P_{N+1} = \frac{1}{\mu}[P_N - \frac{P_N \Psi_{N+1} \Psi_{N+1}^T P_N}{\mu + \Psi_{N+1}^T P_N \Psi_{N+1}}]$$

$$k_{N+1} = \frac{P_N \Psi_{N+1}}{\mu + \Psi_{N+1}^T P_N \Psi_{N+1}}$$

$$e(N+1) = y(N+1) - \Psi_{N+1}^T \hat{a}_N$$

$$\hat{a}_{N+1} = \hat{a_N} + e(N+1)k_{N+1}$$

where $\Psi_{N+1} = [y(N)\ y(N-1)\ ...\ y(N-p+1)]^T$ is the vector containing the past N BG measurements, P is the error covariance matrix and it is initialized to a arbitrarily high initial value, k is the filter gain matrix, e is the prediction residual and $\hat{a}$ is the predicted model state.

3.2.1 Use for basal insulin modulation

In this thesis we will try to use the AR model based predictor in place of the linear predictor used by Patek et al. That is, with reference to equations, 2.22, 2.23 and 2.24 we will substitute $\hat{G}(k)$, calculated with LP, with $\hat{G}_{AR}(k)$, calculated with AR.

Chapter 4

Design and implementation of an in silico scenario to test the modulation algorithms

4.1 Rationale

In order to evaluate the performance of the algorithm already presented in literature we reproduced them inside the Padova/UVA T1D simulator (see section 4.2.1) together with the new innovations proposed in chapter 3 in a Simulink environment. To evaluate their ability to detect and prevent hypoglycemia we simulated some scenarios where a patient erroneous behaviour would induce an hypoglycemic event (see section 4.3). In section 4.4 we report details on the simulink implementation of the implemented algorithms.

4.2 The Padova/UVA T1D simulator

4.2.1 The model

The Padova/UVA T1D simulator [39] is able to simulate a model of the glucose-insulin system in the normal human capable of describing the physiological events which occur during a standard mixed meal.
To derive the simulator parameters a unique meal data set of 204 normal individuals who underwent a triple tracer meal protocol was used, thus allowing to obtain, in a virtually model-independent fashion, the time course of all the relevant glucose and insulin fluxes during a meal.
In figure 4.1 we show the scheme relation of the measured plasma concentrations, i.e., glucose G and insulin I and the glucose fluxes, i.e., rate of appearance Ra, production EGP, utilization U, renal extraction E, and insulin fluxes, i.e., secretion S, and degradation D. The healthy state simulator requires an adaptation to the type 1 diabetes phisiology. In fact it does not have

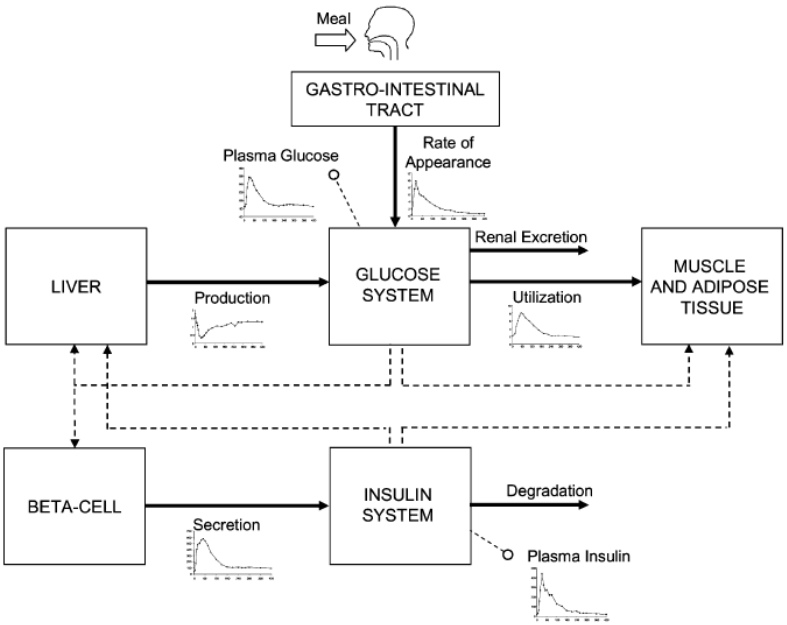

Fig. 4.1: Scheme of the glucose-insulin control system which puts in relation the measured plasma concentrations to glucose fluxes and insulin fluxes.

a beta-cell module resembling the pathologic condition and utilize a model of subcutaneous insulin absorption to simulate the bolus and basal insulin injections. The unit processes of glucose and insulin subsystem are shown in figure 4.2. The model for each of them was identified from average data with a forcing function strategy.
The simulator has a virtual population of 100 adult subjects that have different parameter values to simulate different metabolic characteristics such as glycemic basal value, correction factor etc. For details on the description of every module equations we refer to the original article [39].

4.2.2 The simulink implementation

The simulator is implemented in a MATLAB/Simulink environment. From the main code it is possible to set the different settings to be used in the simulation such as meal amounts and times, virtual subjects population, simulation duration, insulin infusion and glucose infusion.
In figure 4.3 a very high level organization of the simulator is shown. In the "Padova Open Loop" subsystem (labeled as A in the figure) all the operations of insulin injection are calculated accordingly to the simulation settings and their effect is simulated. In this subsystem we implemented our algorithm for basal insulin modulation. The subsystem "meal generator" calculates meals amounts and uses them together with insulin injection information to simulate the metabolic process in the subsystem labeled as C in figure.

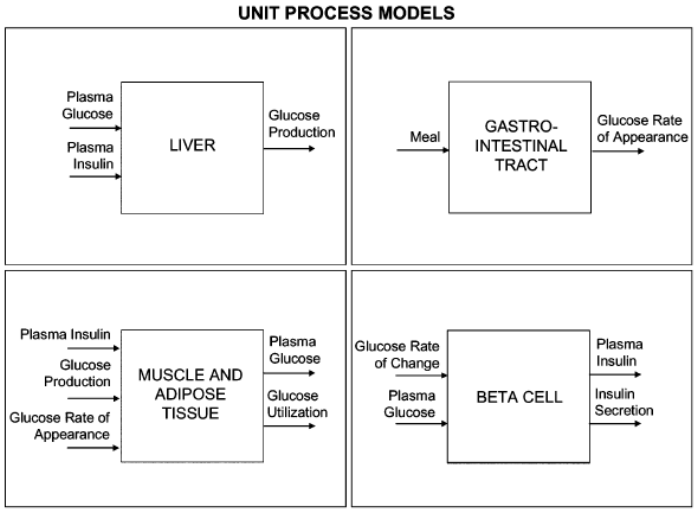

Fig. 4.2: Unit process models and forcing function strategy: endogenous glucose production (top left panel); glucose rate of appearance (top right panel); glucose utilization (bottom left panel); insulin secretion (bottom right panel). Entering arrows represent forcing function variables, outgoing arrows are model output.

The metabolic process is calculated accounting for the set of differential equations described in [39], using a S-function, as shown in figure
The Padova open loop subsystem is shown in figure 4.5. The meal time insulin bolus generator (labeled as A) calculates insulin bolus to be injected at meal time, the insulin correction bolus calculator (B) the post meal correction bolus (when abilitated), the insulin modulation subsystem (C) applies the insulin modulation algorithms.

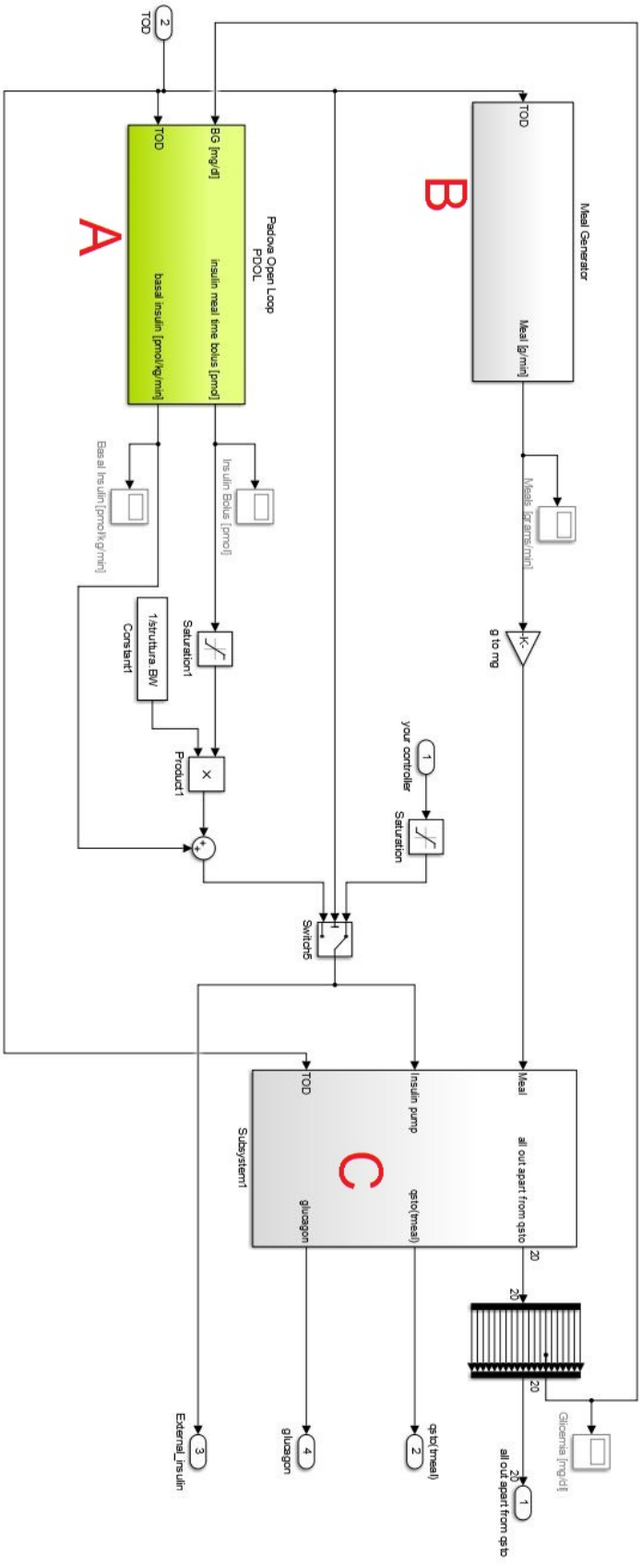

Fig. 4.3: Padova/UVA simulator, simulink view of the "diabetico" subsystem.

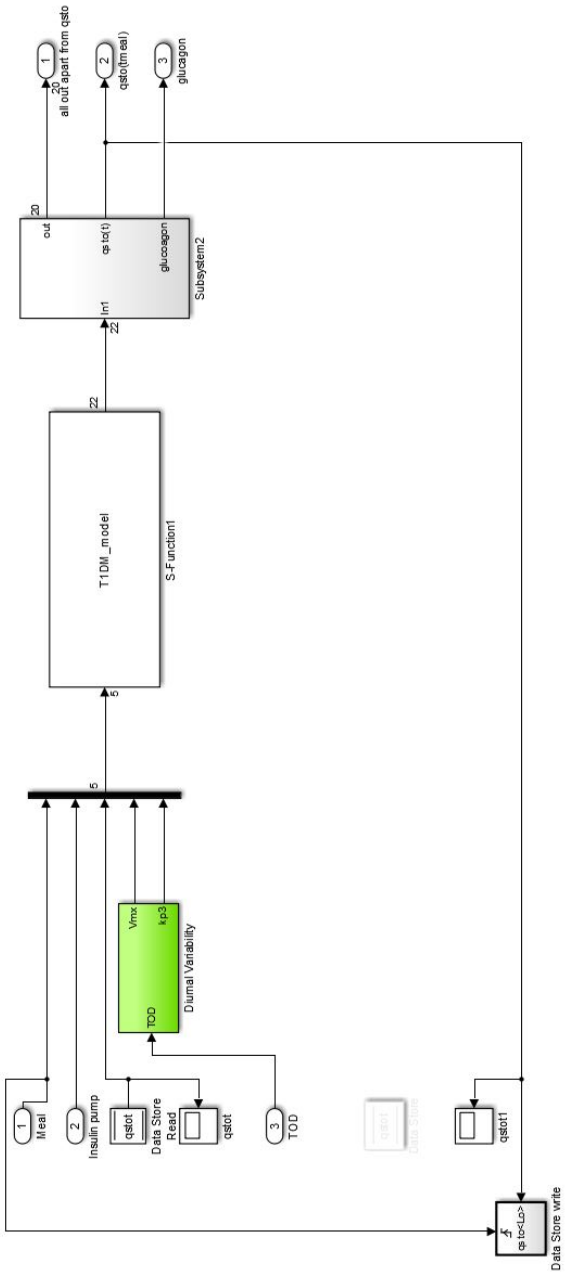

Fig. 4.4: Padova/UVA simulator, simulink view of the metabolic process simulation using a S-function which applies the set of differential equation described in [39].

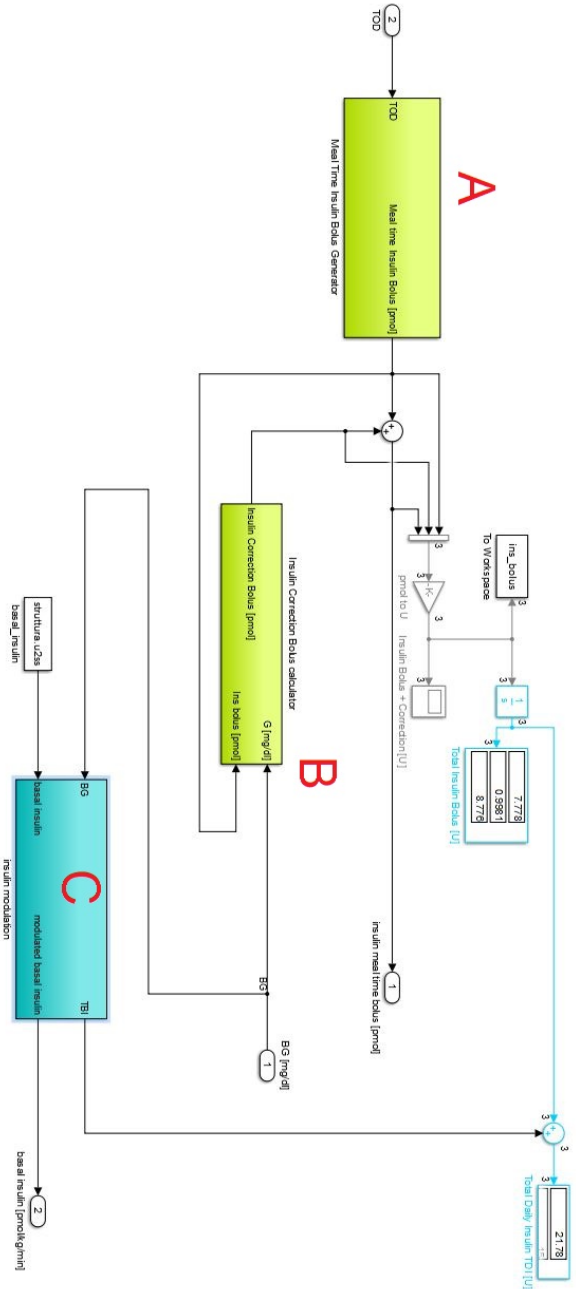

Fig. 4.5: Padova/UVA simulator, simulink view of the Padova open loop subsystem.

4.3 Our simulated scearios

Two different scenarions were implemented to induce hypoglycemia in the virtual subjects. In the first scenario we recreated the same glucose profiles of high variable insulin sensitivity described in the brakes algorithm study whereas in the second we created a more realistic hypoglycemic episodes that could happen in real life e.g. after a meal because of an higher insulin dosing.

4.3.1 Scenario 1: highly variable insulin sensitivity

In their brakes/power brakes article [33], Hughes et al. reported a tentative of simulating a highly variable insulin sensitivity (e.g. after a physical activity). In fact, an increase in insulin sensitivity makes the actual basal insulin delivery rate too high to achieve euglycemia. In theory, the best way to recreate this scenario would be to modify the insulin sensitivity of the virtual patient. However, this results impossible since such a module for rapid and high changes of insulin sensitivity has not been implemented yet. Therefore to achieve such a variation of insulin sensitivity, the authors of the paper [33] delivered twice the amount of normal basal insulin rate to all the 100 subjects, initialized at glucose concentration of 10 mg/dL, to achieve their respecting fasting glucose concentration of 112.5 mg/dL.
In figure 4.6 we can see the BG traces and the average value of the 100 virtual subjects produced during the scenario reproduction which, in our case, was carried out defining the following settings:

- 32 hours long simulation;
- basal insulin delivery doubling happens starting from the 24h time mark and lasts until the end of the simulation;
- since the simulator does not allow to set an initial glucose concentration for the simulation we artificially led the patients blood glucose values to 150 mg/dL using the glucose infusion rate feature of the simulator that delivers a specific glucose amount over time to achieve the desired glucose concentration (150 mg/dL in our case);
- patients basal glucose values were also artifically modified and set to 112.5 mg/dL to mirror the conditions described in the article [33].

4.3.2 Scenario 2: delayed insulin bolus

In the simulator, insulin boluses are calculated optimally therefore it is quite hard to obtain hypoglycemia in a large amount of subjects. As we can see in figure 4.7 A, a sample subject is given a correctly calculated insulin bolus at meal time which happens at 2 hours from the start of the simulation and his

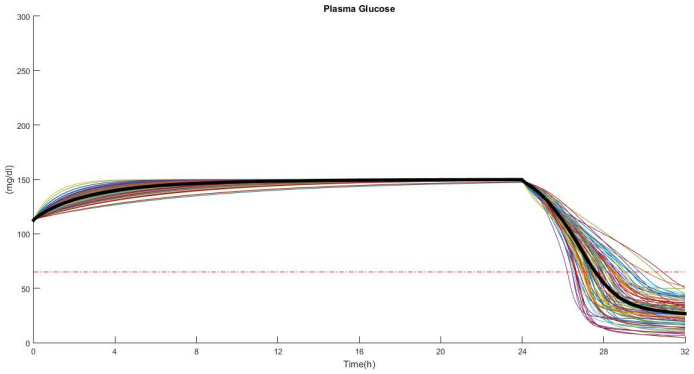

Fig. 4.6: Insulin sensitivity increase scenario: in different colours the BG profiles of the 100 simulator subjects, in black the average BG of them.

BG never crosses the hypoglycemic threshold, here visualized at 65 mg/dL. However, in real-life situations, to perfectly control meal insulin boluses is a hard task as several mistakes can be made such as erroneous carbs estimation, bolus injection time delays or wrong correction boluses injections. In this scenario, we tried to reproduce a situation where a patient assumes a pre-meal insulin bolus for a meal containing 70g of carbs (correctly estimated) but forgets to take it at meal time and injects it 30 minutes afterwards. We will assume that in this scenario the patient is not able to retrieve his pre-meal BG value therefore calculations for the insulin bolus amount will be performed using his BG value at the time of the injection. This erroneous behaviour of the patient is known to cause hypoglycemia and was tested in the simulator with different amount of delay time to achieve the best scenario in which a reasonable amount of subjects would go into hypoglycemia for best results analysis. In figure 4.7 B an example of this scenario is provided. The 30 minutes delay in the bolus injection is enough to cause in the patient an hypoglycemia that lasts for more than two hours if not treated.

4.4 Our simulink implementation

In the open loop module of the Padova/UVA T1D simulator we inserted a section that uses the current BG values computed by other sections of the simulator to calculate the basal insulin attenuation factor through the use of the algorithms described in section 2.3.1, 2.4 and 3.
The implemented solution that is shown in figure 4.8 features:

- A prediction module (figure 4.9), that performs real-time glycemia prediction using either the linear (LP) algorithm or the AR model based (AR) one. Input is current BG value and output is predicted glycemia using the selected PH.

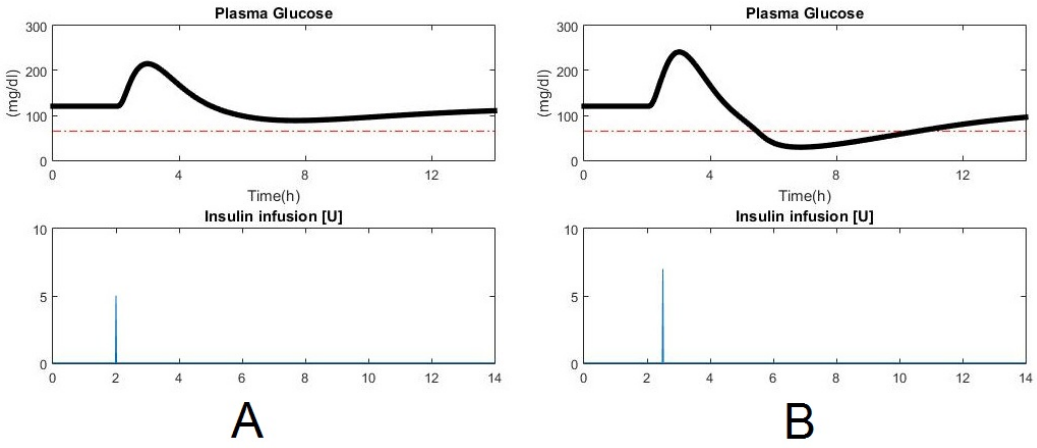

Fig. 4.7: Delayed bolus scenario: A) regular behaviour, no delay in insulin bolus injection; B) injection of meal insulin bolus with 30 a minutes delay.

- An attenuation module (figure 4.10), where the basal insulin attenuation factor is calculated using either the standard risk (SR) or the dynamic risk (DR). Input values are predicted glycemia and current BG to calculate its derivative. In case prediction is disabled the input is current BG. Output value is the attenuation factor to be multiplied to normal basal insulin value.

The simulation settings can be decided using the simulator main code that sets active or inactive different switch controlling:

- CGM noise presence in prediction input (labeled as X in figure 4.8)
- usage of predicted or true BG value (labeled as Y)
- application of insulin modulation or not (labeled as Z)

In the linear prediction module, visualized in figure 4.11, first the unweighted average of the BG values received in $(t-10, t]$ is calculated. Then, using a delay line together with the current BG value, a linear fit is calculated using matlab function polyfit. The angular coefficient is selected from the function output and is multiplied for the PH value and finally summed to the unweighted average BG value to obtain the prediction. The last subsystem before the output recasts the data format and checks for negative values.
The AR prediction module (figure 4.12) uses two memory blocks to memorize the autoregressive model parameters that are updated at every iteration (see section 3.2). The MATLAB function block computes the model parameters and the BG prediction using the current and the last BG values.
In the SR module (figure 4.13), the unweighted average of the BG last 15 values is calculated before the SR and the attenuation factor, calculated using the formula described in [33].

Fig. 4.8: Simulink implementation, contained in the open loop module of the Padova/UVA T1D simulator. Starting from the current BG value (1), a predicted value is calculated (Prediction module A), an attenuation factor is computed (Attenuation module B) and is then multiplied (C) to modulate the patient's basal insulin value (2) and produce a new insulin injection output (3). X, Y, Z are switch determining the usage or not of CGM noise, BG prediction and basal insulin modulation respectively.

The DR module (figure 4.14) calculates SR using the BG as input, it then uses this value, together with the BG current derivative and the $\frac{dr}{dg}$ to compute DR. Finally it is restricted to the 20-120 interval similarly to the brakes formula.

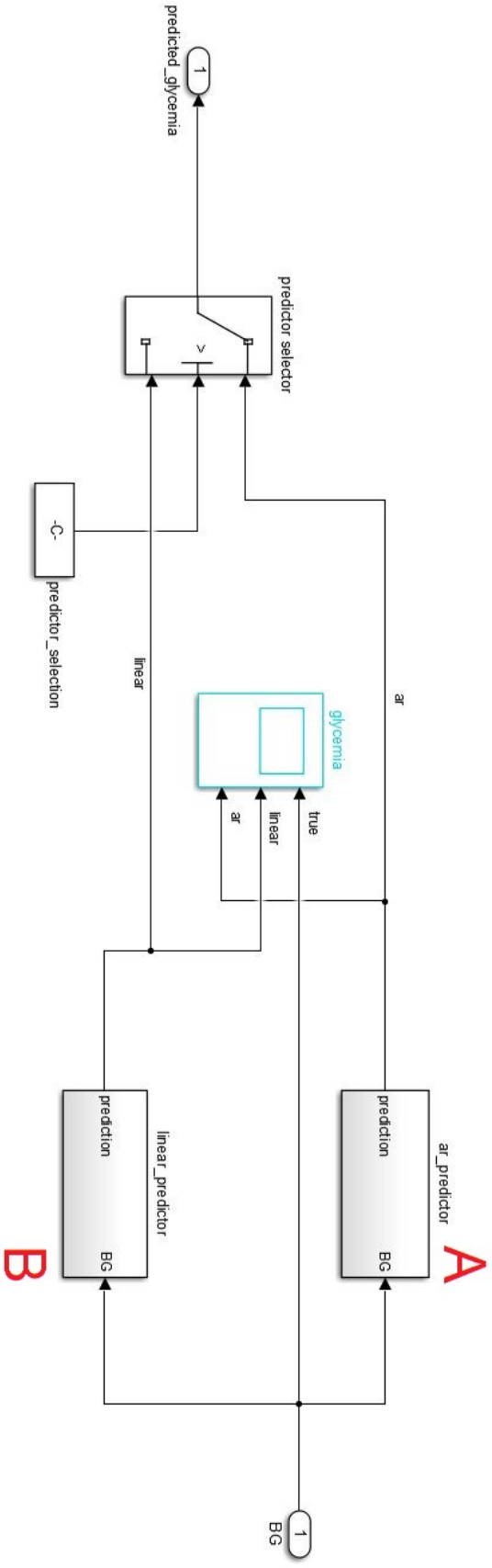

Fig. 4.9: Prediction module, composed by the AR predictor model (A) and the LP predictor module (B)

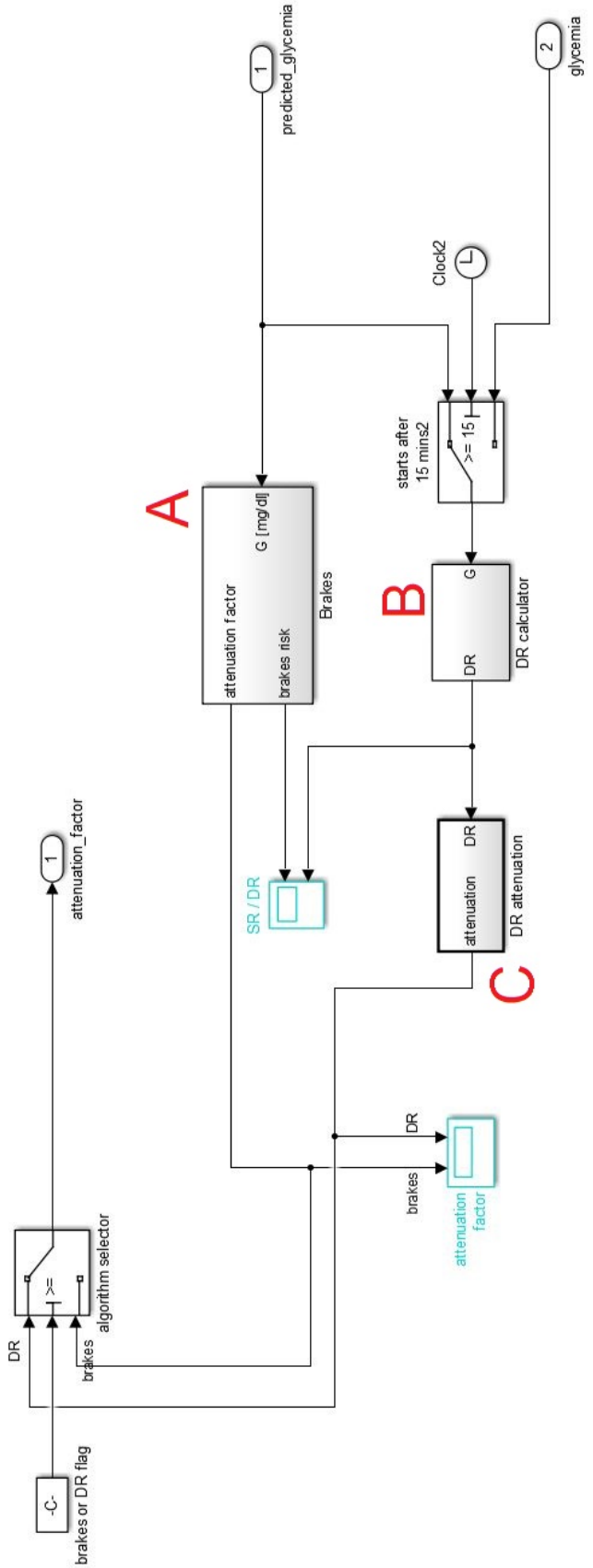

Fig. 4.10: Attenuation module, composed by the brakes module (A), the DR calculator (B) and the DR attenuation module (C).

Fig. 4.11: Linear prediction module: to compute $\hat{G}(k) = \bar{G}(k) + PH \cdot \dot{G}(k)$ we calculate a moving average (A) and the angular coefficient of the linear fit of the last 30 samples using matlab function polyfit (B).

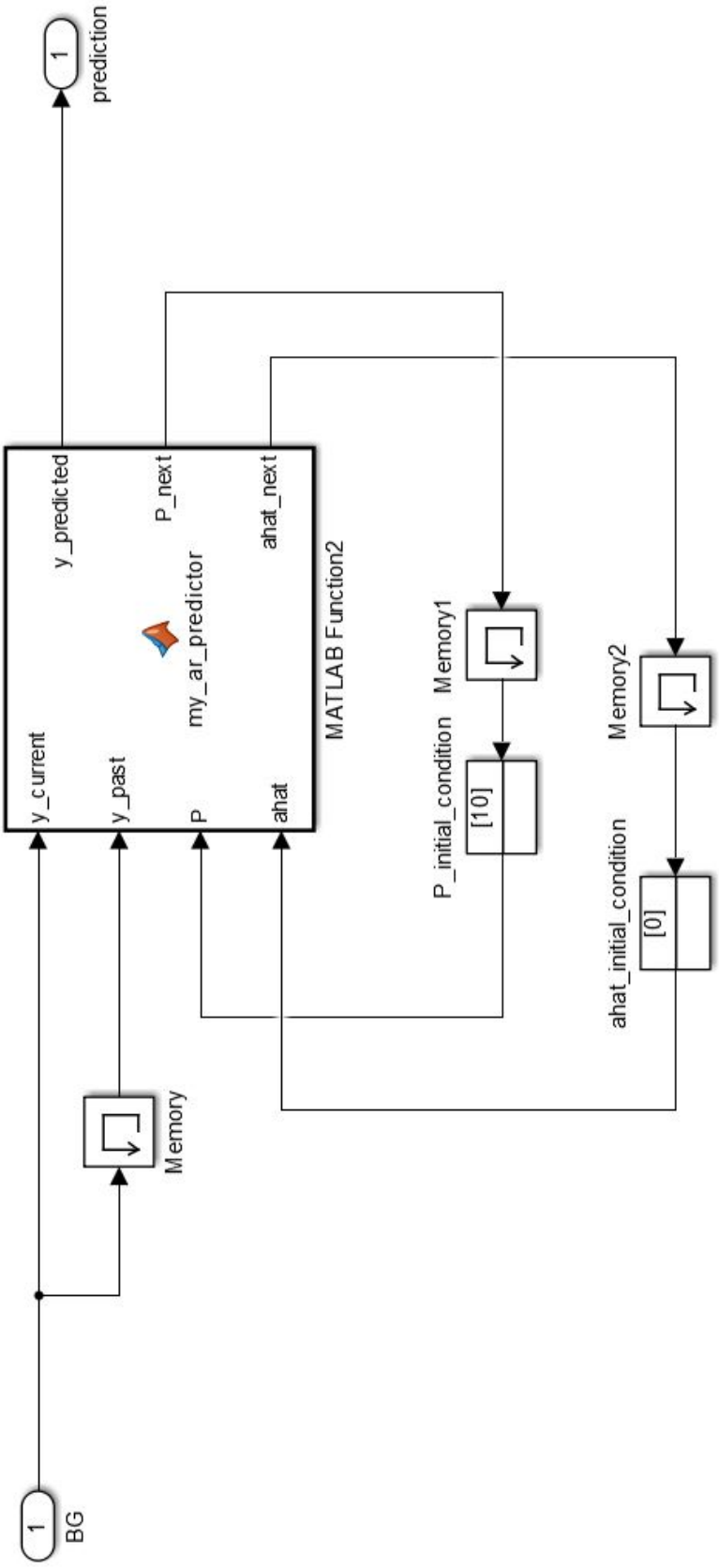

Fig. 4.12: AR prediction module. Model coefficients ($\hat{p}$ and $\hat{a}$) are stored to be readjusted iteratively.

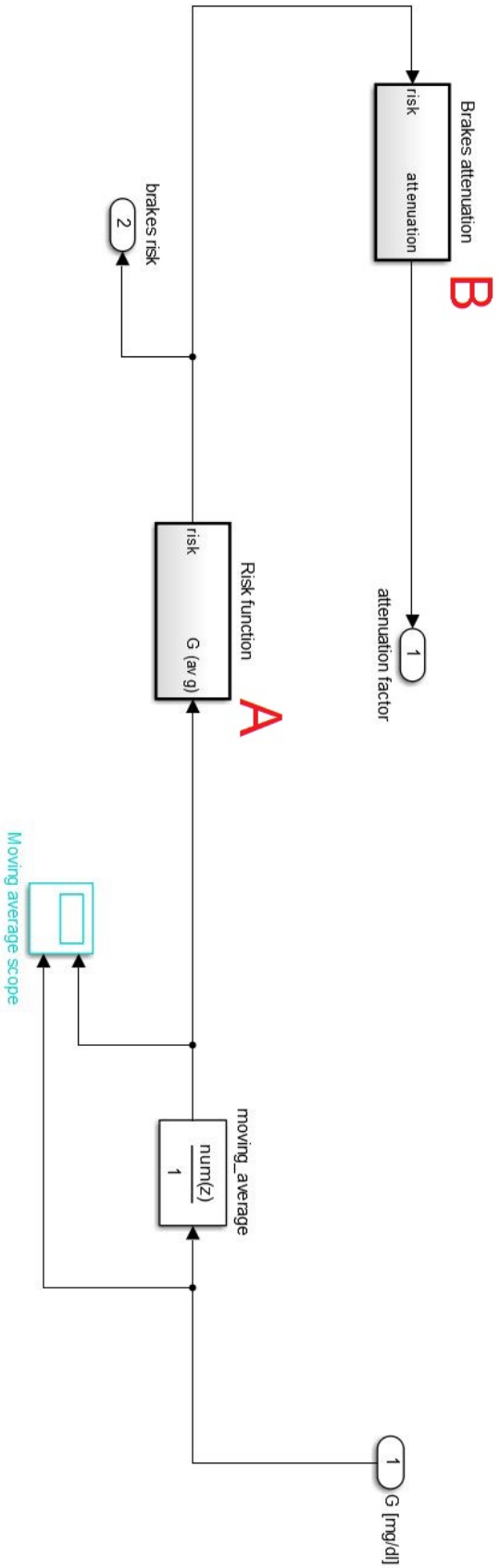

Fig. 4.13: Brakes fed by SR module: SR is computed (A) and then the attenuation factor (B).

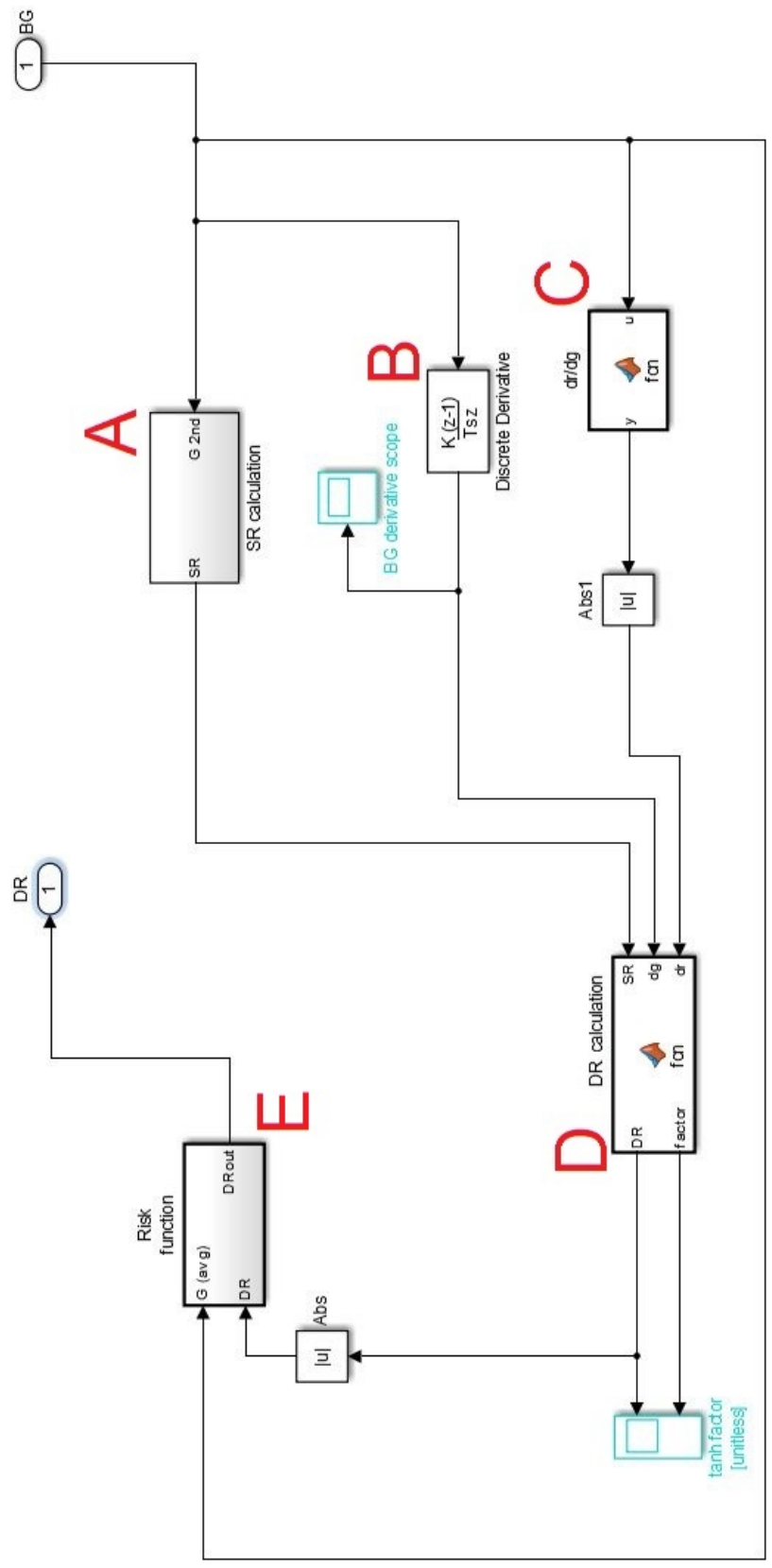

Fig. 4.14: DR module: using calculated SR (A), BG derivative (B) and $\frac{dr}{dg}$ (C), DR can be calculated in (D). The DR risk is restricted to the 20-120 mg/dL interval (E) similarly to brakes.

Chapter 5

Results

We used the simulink implementation described in the previous chapter to try and recreate the results obtained by Hughes et al. with their brakes algorithm using a SR and make a comparison with the results obtained when introducing a linear predictor with different prediction horizon (PH) values (17 and 30 minutes), and when using a DR instead. We then recreated the delayed bolus scenario in which we evaluated the effect of the brakes algorithm compared with the DR when using a linear predictor or an AR model based one, with different PH values.

5.1 Scenario 1: higly variable insulin sensitivity

A visual example of the application of the insulin modulation algorithms to one virtual subject when using modulation calculated with SR or DR and when using different PH. can be seen in figure 5.1 and 5.2.
In figure 5.1a and 5.2a we can see that as insulin delivery rate is doubled the example virtual subject BG drops into hypoglycemia. The application of the SR based basal insulin modulation algorithms (figure 5.1b) gradually lower the basal insulin delivery when BG value begins to fall into the hypolgycemic area, until reaching a value close to zero. As soon as the BG derivative assumes a positive value, insulin modulation ceases and basal delivery rate returns to its previous value. In order to evaluate the algorithms performances we will not analyze the following BG oscillations and insulin suspension that are cause to maintenance of the doubled insulin value in this scenario. The application of the DR makes so that the insulin modulation process is moved up and attenuation is performed more rapidly. Again the basal insulin delivery rate value reaches a value very close to zero and then normal delivery is restored gradually as soon as the patient starts moving away from the hypoglycemic zone.

In figure 5.3 we can visualize the results obtained on all the 100 virtual sub-

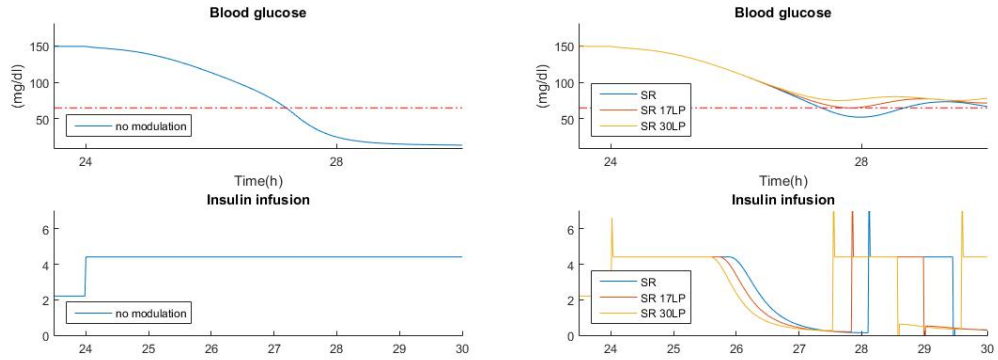

(a) no prediction (b) 17min prediction

Fig. 5.1: Highly variable insulin sensitivity scenario: BG and insulin infusion when not using insulin modulation (a) and when using SR based insulin modulation with and without prediction (b). Example on 1 virtual subject.

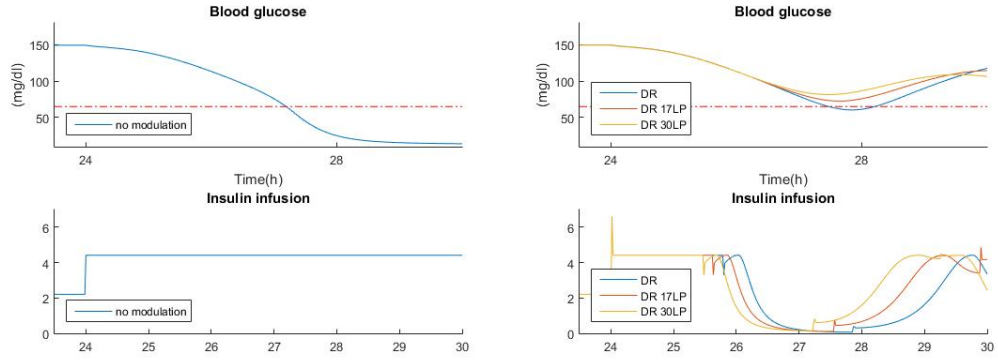

(a) SR (b) DR

Fig. 5.2: Highly variable insulin sensitivity scenario: BG and insulin infusion when not using insulin modulation (a) and when using DR based insulin modulation with and without prediction (b). Example on 1 virtual subject.

jects. After the initial period where all subjects are brought to a glucose concentration of 150 mg/dL, the doubling of the basal insulin infusion (happening at 24h) would cause severe hypoglycemia in the entirety of the subjects as one would observe in figure 5.3a. When applying the Brakes fed by SR algorithm a noticeable improvement can be seen in the average BG value (black) although many patients (coloured traces) still experience severe hypoglycemia for prolonged time. The introduction of DR, as we can see in figure 5.3c, lowers the amount of patients experiencing hypoglycemia compared to when using a SR, however is still not able to perform a good prevention in many cases. The difference in behavior during the recovery phase between SR and DR is due to the risk formulation. The SR sets risk equal to zero when the BG derivative is not negative that happens during the recovery phase while the DR formulation that we provided already produces a different risk behaviour during the "fall" and the "rise" phases.

This difference results in a faster recovery together with a bigger "rebound effect" in BG values after the insulin modulation when using DR. Using a 17 min PH (figures 5.3d and 5.3e) produces a big reduction of the number of patients experiencing hypoglycemia. However, when using SR, some patients are not able to recovery through the applied basal insulin modulation and remain under the hypoglycemic threshold. With the same PH, the use of DR is able to successfully make all the patients recover from the hypoglycemic area, although some of them still experience hypoglycemia for a period of time. The modulation performed by using a 30 min PH (figures 5.3f and 5.3g) seems to provide the better prevention, especially when using the DR, in which case only one patient seems to cross the hypoglycemic threshold.

In figure 5.4 we report the results showing average BG value and SD deviation for the 100 simulator subjects again when using SR/DR and with different PH. We can again observe that without the usage of the insulin modulation algorithm the totality of the subjects would go and remain in hypoglycemia. Brakes fed by SR are effective on average BG values but not as much for a considerable portion of subjects, here visualized by the lower double SD curve. DR introduces an improvement by increasing the minimum BG values reached by the patients but is still unable to provide complete prevention. The "rebound" effect is here seen not to cause hypoglycemia even in extreme cases (higher double SD curve). The usage of a 17 min prediction seems to be effectively move up the basal insulin modulation in time for hypoglycemia prevention in the majority of the cases. By extending the PH to 30 min even better results are achieved especially when using DR where the lowest SD curve seems to never cross the hypoglycemic threshold.

From a distinct comparison between the average BG values displayed in figure 5.5a we can see that when BG value is approaching the hypoglycemia region, DR is able to detect effectively a higher risk in the patient situation resulting in a faster basal insulin attenuation and a higher average minimum BG value in the simulator subjects.

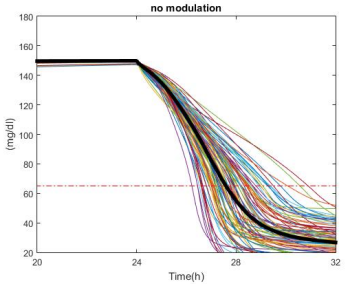

(a) no modulation

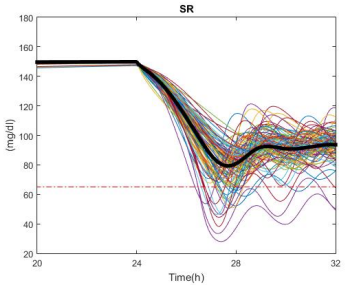

(b) SR

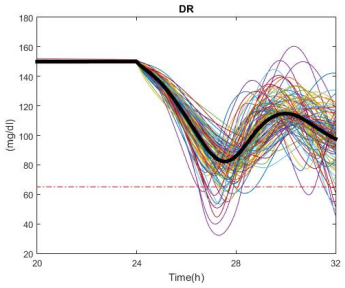

(c) DR

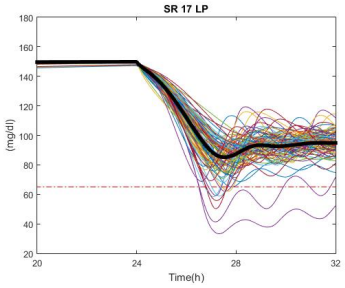

(d) SR with 17m prediction

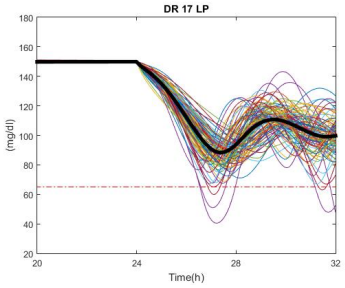

(e) DR with 17m prediction

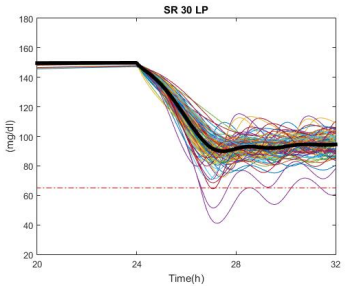

(f) SR with 30m prediction

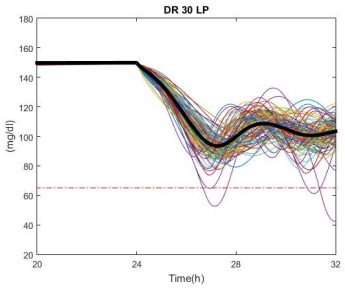

(g) DR with 30m prediction

Fig. 5.3: Single BG values and average value (black) of the 100 virtual simulator subjects in the highly variable insulin sensitivity scenario.

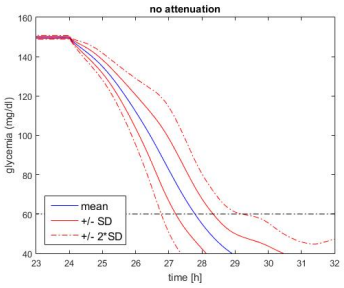

(a) no modulation

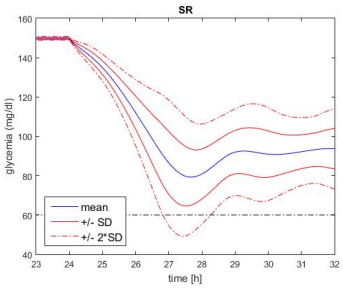

(b) SR

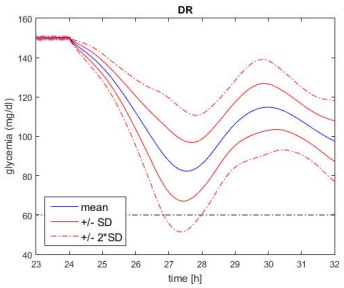

(c) DR

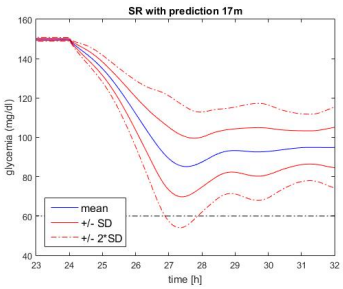

(d) SR with 17m prediction

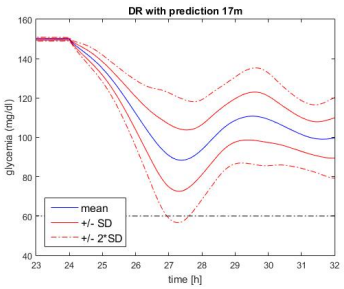

(e) DR with 17m prediction

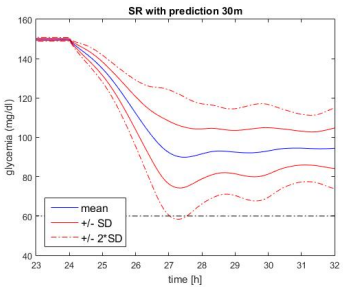

(f) SR with 30m prediction

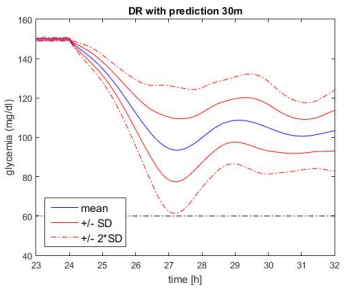

(g) DR with 30m prediction

Fig. 5.4: Average BG value (100 subjects) in highly variable insulin sensitivity scenario. Blue trace represents average BG and red traces single (straight line) and double (dashed) standard deviation values.

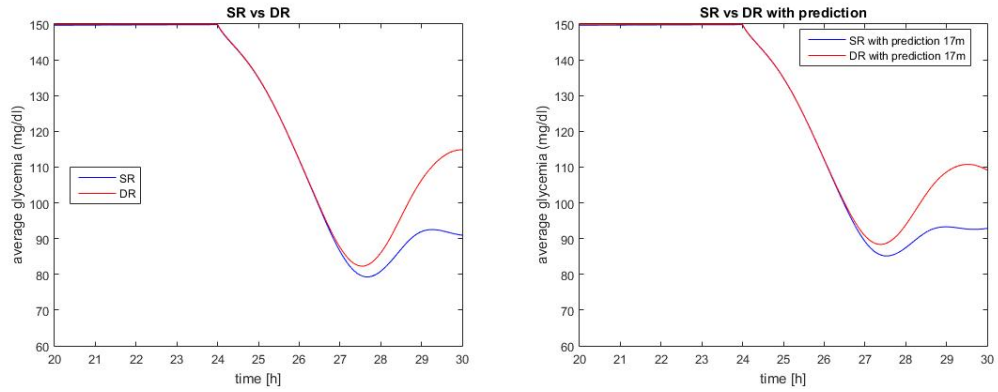

(a) no prediction (b) 17min prediction

Fig. 5.5: Comparison between SR (blue) and DR (red). Average values (100 subjects).

In figure 5.5b the same behaviour is observed even when using a prediction algorithm and higher BG values are maintained. The lengthening of the PH also produces an advance in the time of activation of the insulin modulation resulting in better prevention both when using a SR and a DR (figure 5.6a and 5.6b).

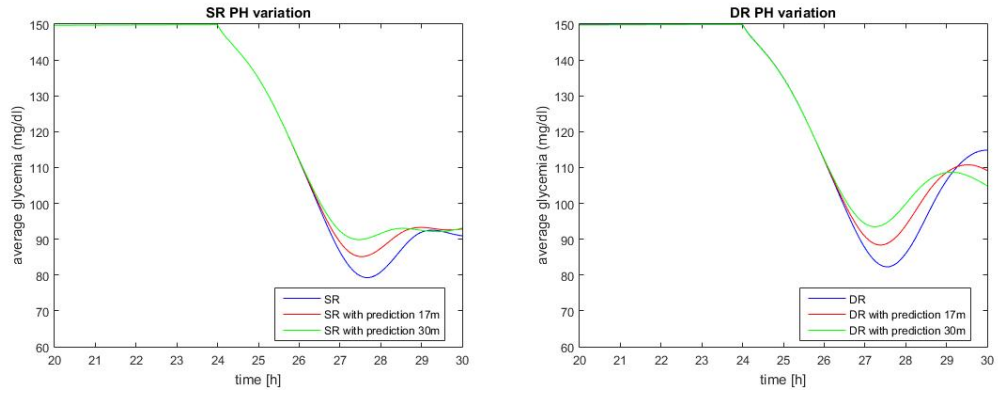

(a) SR (b) DR

Fig. 5.6: Prediction horizon increase effect in SR and DR with no prediction (blue), 17 min prediction (red), 30 min prediction (green). Average values (100 subjects).

In table 5.1 the statistical results concerning the amount of hypoglycemic cases are shown for different hypoglycemic thresholds (70, 60 and 55 mg(dL). As we can see, without using any modulation algorithm every subjects experience hypoglycemia. The usage of modulation based on SR is effective in general but still fails to prevent in 30% of the cases considering an hypoglycemic threshold of 70 mg/dL. DR improves the performance, lowering the

unsuccessful cases to 20%. The 17 min prediction produced a further lowering of the amount of subjects with a BG value below 70 mg/dL, with only 3 subjects below 55 mg/dL. The lengthening of the prediction horizon from 17 to 30 minutes produced a serious improvement in number of prevented cases. Using a 30 min PH prediction we managed to obtain a almost total prevention of hypoglycemic events with except for a couple of patients.

	70 mg/dL	**60 mg/dL**	**55 mg/dL**
no modulation	100	100	100
SR	31	16	12
DR	20	11	8
SR 17 min prediction	14	7	3
DR 17 min prediction	9	3	2
SR 30 min prediction	4	2	2
DR 30 min prediction	2	1	1

Table 5.1: Hypoglycemic events statistics: number of subjects with a least a BG value below 70/60/55 mg/dL.

5.2 Scenario 2: delayed insulin bolus

We tried to simulate a scenario in which the patient does not perform a BG measure before a meal (containing 70 grams of carbs) to calculate the adequate insulin bolus. He then proceeds to measure his BG with a definite time amount of delay following the meal and accounts the insulin bolus amount accordingly to that measurement.

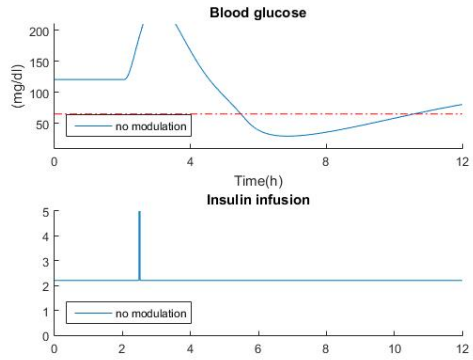

(a) no modulation

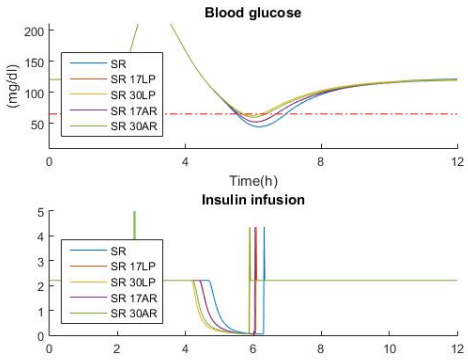

(b) SR

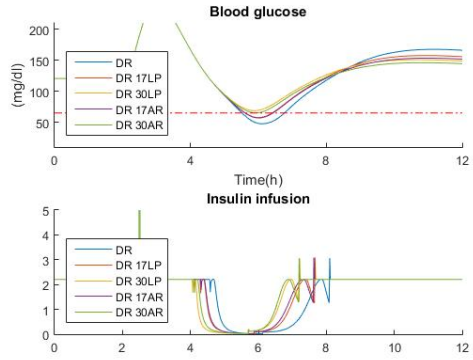

(c) DR

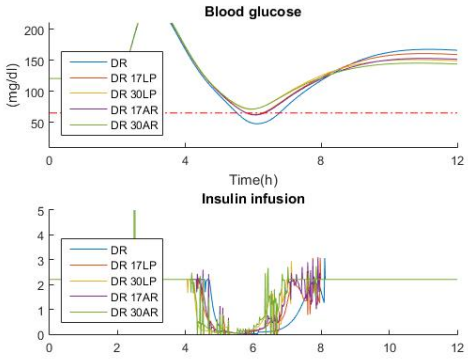

(d) DR (with noise)

Fig. 5.7: Delayed insulin bolus scenario: BG and insulin infusion when not using insulin modulation (a) and when using SR (b) or DR (c) based insulin modulation with and without prediction and with noise (d). Example on 1 virtual subject.

A preliminar analysis was performed to evaluate the adequate amount of time delay that would provide the most interesting statistical distribution regarding the number of hypoglycemia cases induced on the population and the one that would be considered reasonably realistic. Following different tries we decided to use the value of 30 minutes.
In this scenario we evaluated again the efficacy of the brakes algorithm in preventing hypoglycemia when using a SR or a DR and when using two different prediction algorithm, linear prediction (LP) or ar model based (AR),

with different prediction horizons (PH).
Finally we used a CGM noise model described by Facchinetti et al. in [40] in addition to the BG signal in input to the prediction module and evaluated the different algorithms performance.
An example of the application of the basal insulin modulation algorithms is shown in figure 5.7 for one example virtual subject. Compared to when not using insulin modulation (figure 5.7a), SR (figure 5.7b) is able to reduce the time spent in hypoglycemia by inducing a reduction of the delivery rate of basal insulin for a duration of 2 hours. DR based insulin modulation (figure 5.7c also appears effective to reduce the time spent in hypoglycemia and to prevent it completely when using a 30 min prediction even when considering CGM noise (figure 5.7d).

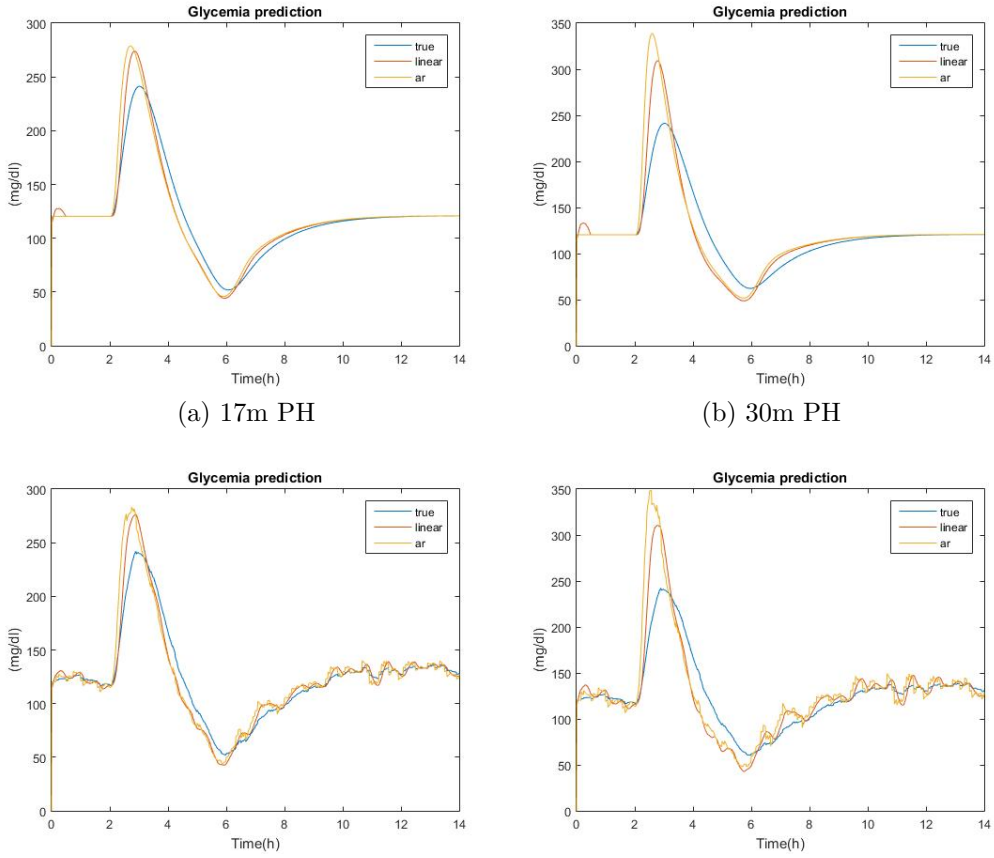

(a) 17m PH (b) 30m PH

(c) 17m PH with CGM noise (d) 30m PH with CGM noise

Fig. 5.8: Example of glycemia prediction (with and without CGM noise) in one patient using LP (red) or AR (yellow). True BG value is shown in blue.

In figure 5.8 an example of the prediction performed with LP and AR with and without CGM signal noise is shown on one virtual patient. We can see that both algorithms are able to predict efficiently the glucose trend and that the prediction is effectively in advance of the true value signal by the value of

the PH. Both algorithms predict a bigger peak of BG value than the true one at meal time, and a slight lower value of BG in the descending phase of the BG curve, after meal. Even when in presence of noise, as shown in figure 5.8c and 5.8d, both algorithms seem to be able to provide a quite good estimation of the BG trend.
Simmetrically to scenario 1, we report the results for the 100 virtual subjects in figure 5.9 and figure 5.10. We also show in figure 5.9 and 5.10 the calculated average and SD. We can see that, when using DR, the average value does not go below the 60 mg/dL threshold and the recovery phase resolves quicker. Observing the results produced by the use of LP and AR prediction algorithms we can say that both prediction are able to effectively influence the prevention of hypoglycemia in average.
We also report some comparisons using only average BG values of the 100 subjects. In figure 5.13a and 5.13b we can see again just like in the previous scenario that DR is able to prevent hypoglycemia more efficiently than SR.
The difference of performance between the LP and the AR predictor when using a 17m PH is barely visible, when using a 30m PH, the LP predictor shows a small advantage (see figures 5.14a and 5.14b)
The increase of the prediction horizon provides better hypoglycemia prevention both when using LP (figure 5.15a) and when using AR (figure 5.15b).

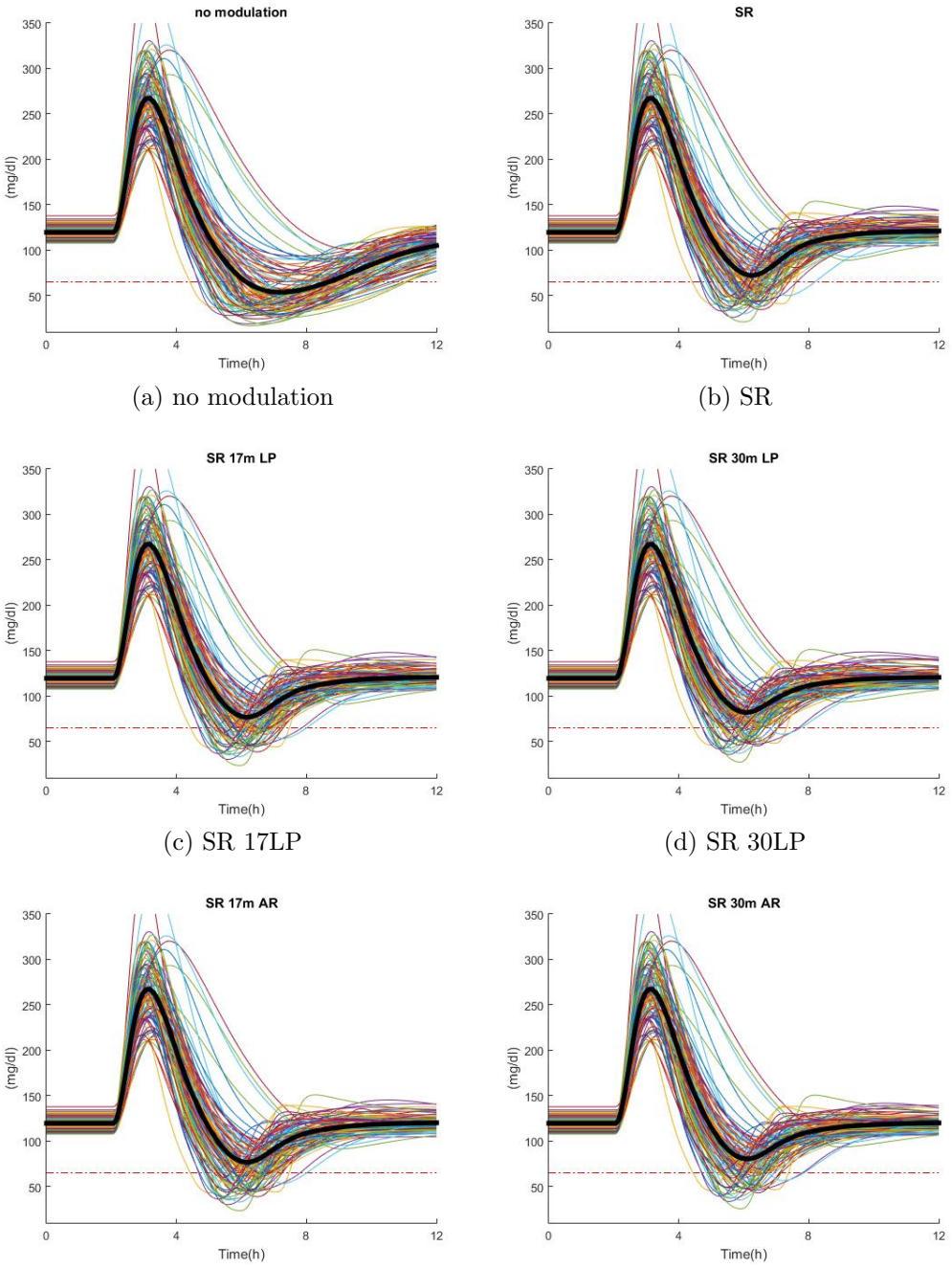

(a) no modulation (b) SR

(c) SR 17LP (d) SR 30LP

(e) SR 17AR (f) SR 30AR

Fig. 5.9: Single BG values and average value (black) of the 100 virtual simulator subjects in the highly variable insulin sensitivity scenario. SR based insulin modulation.

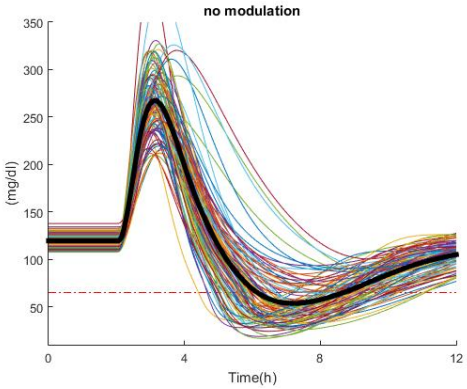

(a) no modulation

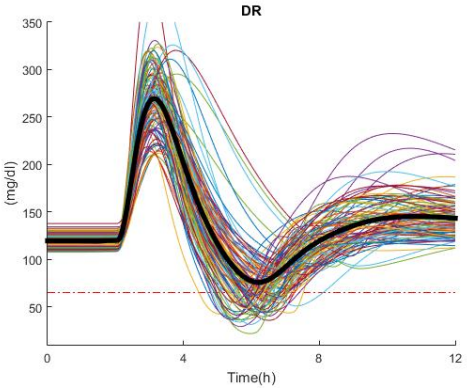

(b) DR

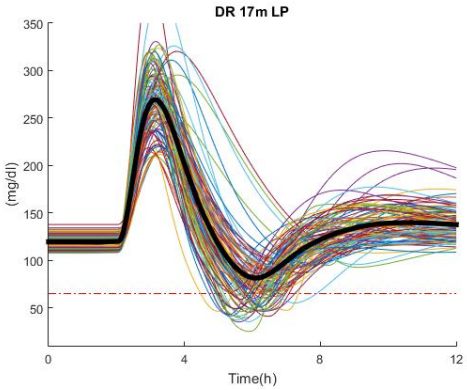

(c) DR 17LP

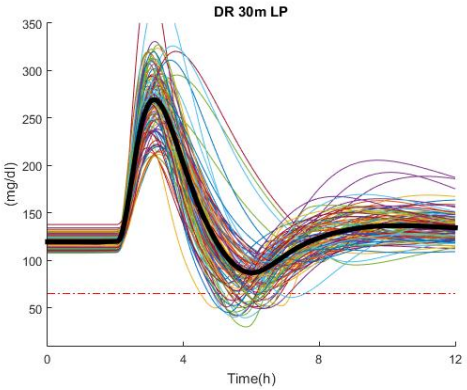

(d) DR 30LP

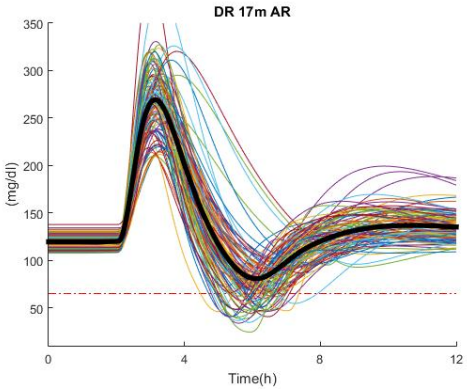

(e) DR 17AR

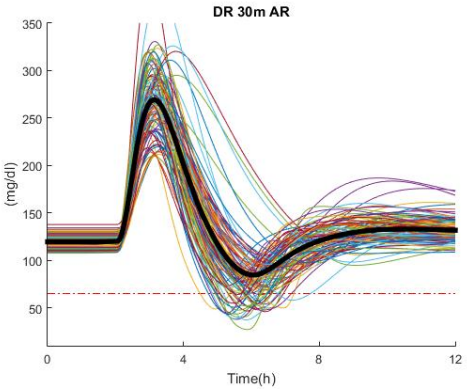

(f) DR 30AR

Fig. 5.10: Single BG values and average value (black) of the 100 virtual simulator subjects in the highly variable insulin sensitivity scenario. DR based insulin modulation.

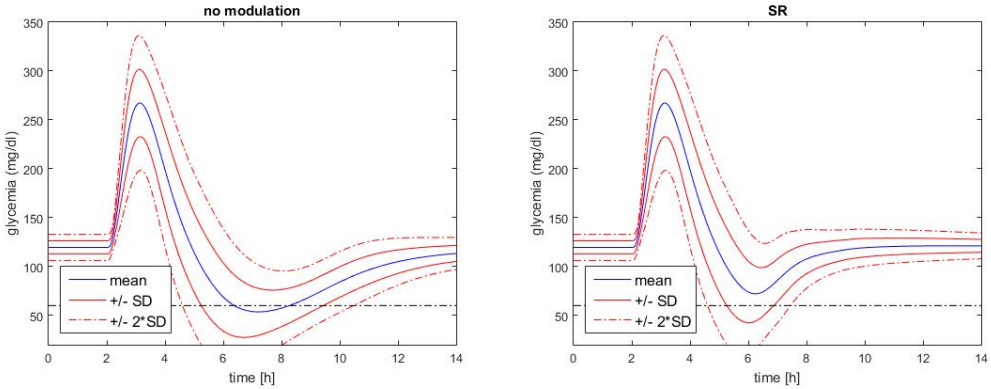

(a) no modulation

(b) SR

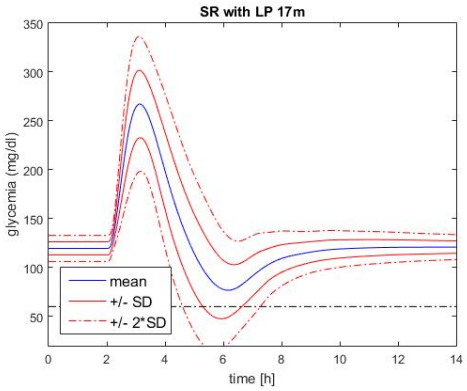

(c) SR 17LP

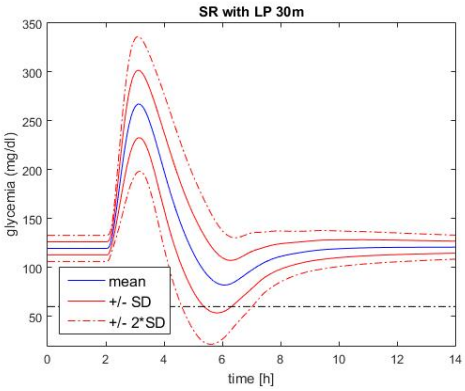

(d) SR 30LP

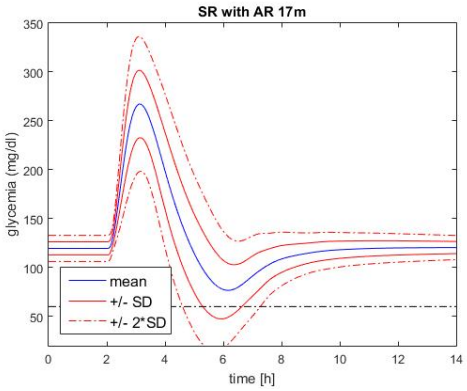

(e) SR 17AR

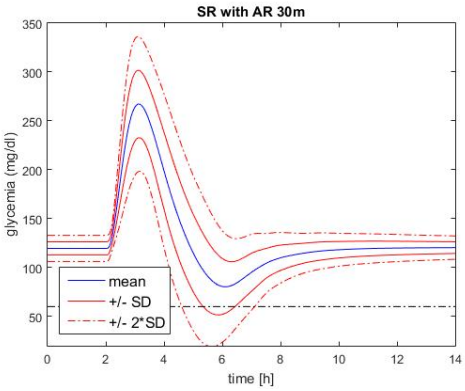

(f) SR 30AR

Fig. 5.11: Average BG value (100 subjects) in delayed insulin bolus scenario. Blue trace represents average BG and red traces single (straight line) and double (dashed) standard deviation values.

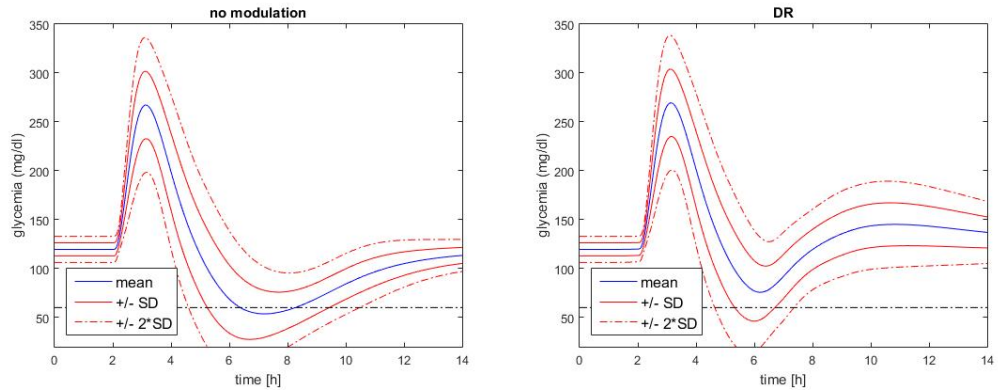

(a) no modulation

(b) DR

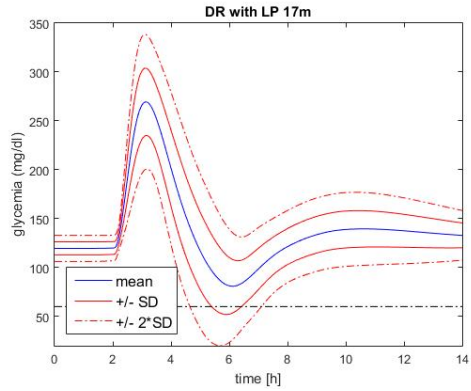

(c) DR 17LP

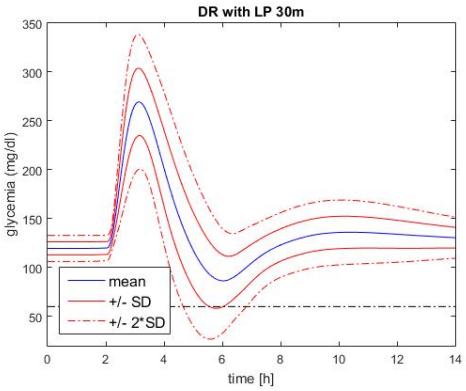

(d) DR 30LP

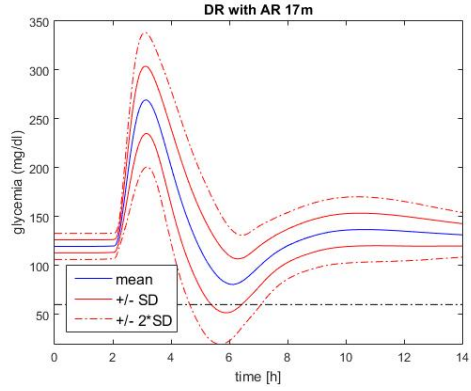

(e) DR 17AR

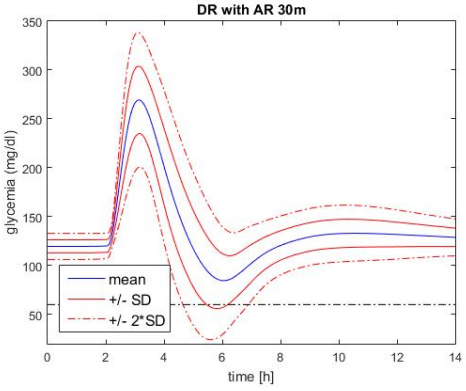

(f) DR 30AR

Fig. 5.12: Average BG value (100 subjects) in delayed insulin bolus scenario. Blue trace represents average BG and red traces single (straight line) and double (dashed) standard deviation values.

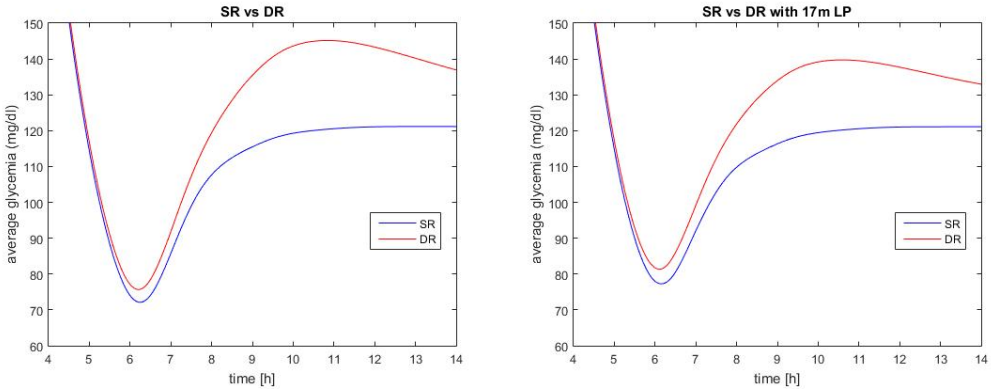

(a) no prediction (b) 17m LP

Fig. 5.13: Comparison between SR and DR when not using prediction (a) and when using 17m PH LP. Average value (100 subjects).

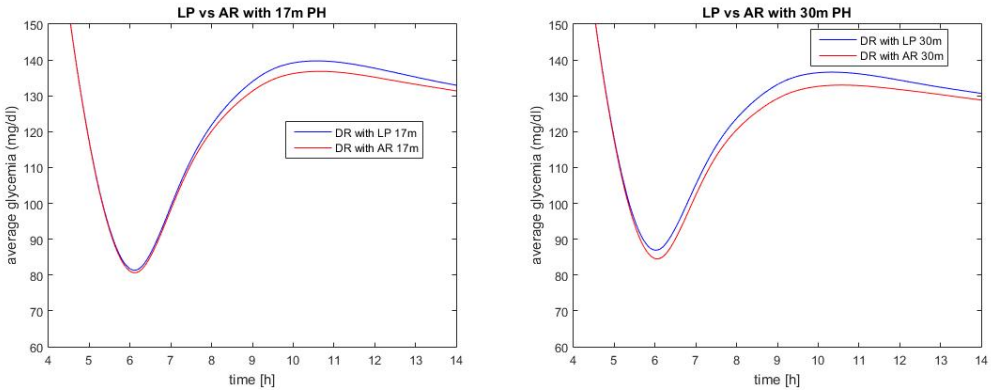

(a) 17m PH (b) 30m PH

Fig. 5.14: Comparison between LP and AR prediction with 17m (a) and 30m (b) prediction horizon. Average value (100 subjects).

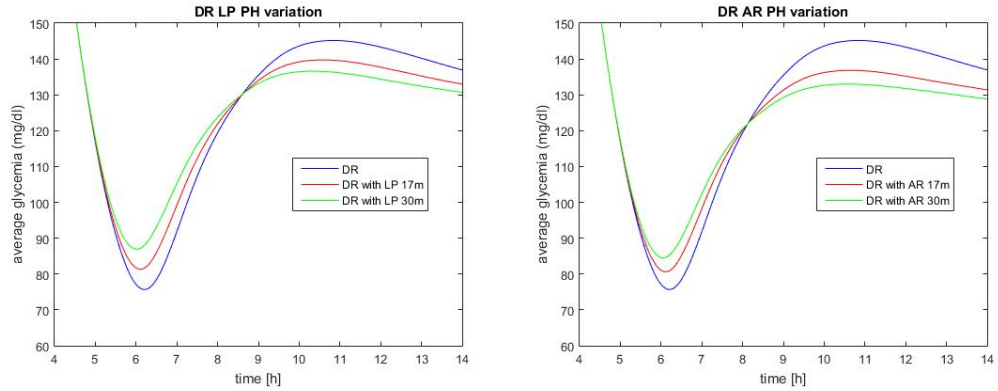

(a) 17m PH (b) 30m PH

Fig. 5.15: Effect of increasing PH when using LP (a) or AR (b). Average value (100 subjects).

In the previous scenario the totality of the subjects experienced extremely low BG values for a very prolonged time and therefore virtual death. This scenario instead represents a more realistic scenario where all the subjects, with different times, naturally recover from the hypoglycemic state. Therefore we cannot easily evaluate the algorithms efficacy just by looking at the graphic results of the 100 virtual subjects combined. Unlike a normal scenario where no bolus delay is applied (see table 5.2) almost the entirety of the subjects (70-80%) experience mild or severe hypoglycemia in this scenario.
In order to perform a more thorough analysis we went on calculated together with the number of hypoglycemia cases similarly to scenario 1, the average time that a patient would spend with a BG value under the 70, 60 and 50 mg/dL thresholds. Together with this data we calculated the number of subjects that during the simulation spent a time higher than 60, 90 and 120 minutes below the 70, 60 and 50 mg/dL threshold.

	70 mg/dL	**60 mg/dL**	**55 mg/dL**
Normal	6	2	0
30m bolus delay	82	74	72

Table 5.2: Number of subjects that experience BG values below 70/60/55 mg/dL, normal scenario and bolus delay.

In table 5.3 and 5.4 we report the statistics relatively to the percentage of single cases prevented. We can see that overall DR is better than SR at preventing hypoglycemia as it provides better results in every scenario. For example severe hypoglycemic cases (below 55 mg/dL) went from 47 using SR to 36 using DR. Introducing prediction algorithms resulted in better prevention and raising the prediction horizon increased the positive effect as well. Using DR with a 17 minutes prediction algorithm the percentage of subjects below 70 mg/dL went from 70% (normal case) to 50%. Increasing the prediction horizon to 30 minutes lowered this percentage to around 30%. AR prediction provided overall sligthly worse results than LP. This difference goes to almost unnoticed in the 70 mg/dL threshold result to a $\sim$5% difference in the 50 mg/dL threshold. The introduction of CGM noise in the prediction input module resulted in a overall slightly higher amount of prevented cases. This may be due to possible lower than normal BG values detected that triggered the risk function thus the attenuation in advance and resulted in higher basal insulin attenuation.
Results when using SR and DR are shown in tables 5.5 and 5.6 respectively. Once again DR shows better results than SR in every aspect. The average time below 70mg/dL is reduced from 53% to 43% and the amount of subjects below 70mg/dL for more than 60min is reduced from 50 to 35 when no prediction is applied. The implementation of a prediction algorithm together with the DR was effective both when using LP and AR, the average time below 55 mg/dL is decreased by 50% when using a 17m PH and is halved when using

a 30m PH. The comparison between LP and AR is somewhat in favor of the LP, consistently scoring lower average times and number of subjects in hypoglycemia although with very little difference. The introduction of CGM noise seems again to produce better results in hypoglycemia prevention but this result can be attributed to erroneous lower than true BG values which trigger the risk function in advance. Encouraging results can be observed when using a DR with any predictor and a 30min PH: the totality of the subjects does not spend a time higher than 90 minutes below the 60 mg/dL threshold.

	70 mg/dL	**60 mg/dL**	**55 mg/dL**
no modulation	82	74	72
SR	71	57	47
SR (noise)	71	57	47
SR AR 17m	66	42	32
SR LP 17m	65	39	32
SR AR 17m (noise)	60	38	29
SR LP 17m (noise)	59	36	29
SR AR 30m	54	31	27
SR LP 30m	45	28	23
SR AR 30m (noise)	48	29	26
SR LP 30m (noise)	43	27	21

Table 5.3: Number of subjects with a BG value under 70/60/55 mg/dL in delayed bolus scenario, SR attenuation.

	70 mg/dL	**60 mg/dL**	**55 mg/dL**
no modulation	82	74	72
DR	68	45	36
DR (noise)	68	45	36
DR AR 17m	54	31	28
DR LP 17m	53	31	26
DR AR 17m (noise)	53	30	26
DR LP 17m (noise)	55	30	26
DR AR 30m	37	25	23
DR LP 30m	33	24	18
DR AR 30m (noise)	35	25	21
DR LP 30m (noise)	32	22	18

Table 5.4: Number of subjects with a BG value under 70/60/55 mg/dL in delayed bolus scenario, DR attenuation.

	70mg/dL				60mg/dL				55mg/dL			
	AVG	**60m**	**90m**	**120m**	**AVG**	**60m**	**90m**	**120m**	**AVG**	**60m**	**90m**	**120m**
no attenuation	180,12	82	79	74	136,28	73	71	63	115,3	68	62	56
SR no prediction	53,38	50	19	3	33,75	26	7	0	24,83	19	3	0
SR AR 17m	42,52	34	14	3	23,28	20	5	1	17,48	13	2	0
SR LP 17m	41,18	34	13	3	22,32	18	4	1	16,77	10	2	0
SR AR 17m (noise)	38,97	32	13	2	21,36	16	2	0	15,73	12	1	0
SR LP 17m (noise)	37,52	32	12	2	20,3	14	2	0	14,95	11	1	0
SR AR 30m	32,78	26	10	2	18,01	15	3	0	13,48	8	1	0
SR LP 30m	26,78	23	5	1	14,88	10	1	0	10,77	6	0	0
SR AR 30m (noise)	30,76	26	10	1	16,45	12	1	0	11,9	8	1	0
SR LP 30m (noise)	27,79	22	6	1	14,7	11	1	0	10,43	8	0	0

Table 5.5: SR hypoglycemia statistics: average (AVG) time (minutes) spent by the subjects with a BG value below 70/60/55 mg/dL and number of subjects with a BG values below 70/60/55 mg/dL for a period of time bigger than 60/90/120 minutes.

	70mg/dL				60mg/dL				55mg/dL			
	AVG	**60m**	**90m**	**120m**	**AVG**	**60m**	**90m**	**120m**	**AVG**	**60m**	**90m**	**120m**
no attenuation	180,12	82	79	74	136,28	73	71	63	115,3	68	62	56
DR no prediction	43,79	35	13	2	25,24	23	3	0	18,86	13	0	0
DR AR 17m	31,11	26	6	1	17,41	12	2	0	13,2	8	0	0
DR LP 17m	30,67	26	6	1	17,12	12	2	0	12,75	8	0	0
DR AR 17m (noise)	30,61	25	7	1	16,56	10	1	0	12,28	7	0	0
DR LP 17m (noise)	30,34	24	4	0	16,2	9	1	0	11,75	6	0	0
DR AR 30m	22,9	23	3	0	13,4	9	0	0	9,72	5	0	0
DR LP 30m	19,99	17	3	0	11,36	7	0	0	7,58	3	0	0
DR AR 30m (noise)	21,31	21	3	0	12,31	8	0	0	8,6	4	0	0
DR LP 30m (noise)	18,33	14	2	0	9,95	6	0	0	6,53	3	0	0

Table 5.6: DR hypoglycemia statistics: average (AVG) time (minutes) spent by the subjects with a BG value below 70/60/55 mg/dL and number of subjects with a BG values below 70/60/55 mg/dL for a period of time bigger than 60/90/120 minutes.

Chapter 6

Conclusions

Continuous glucose monitoring is a promising tool in type 1 diabetes treatment especially when combined with insulin pump to provide basal insulin delivery rate modulation.

In this thesis we created a simulink environment starting from the Padova/UVA type 1 diabetes simulator in which we could test different algorithms for basal insulin modulation. In particular we were able to successfully recreate a scenario in which hypoglycemia is induced in patients to simulate a highly variable insulin sensitivity situation (scenario 1), as proposed by Hughes et al. [33] and we created a more realistic scenario of hypoglycemia by simulating a delayed meal insulin bolus situation (scenario 2). We managed to reproduce an algorithm for basal insulin modulation based on a standard risk function and to test its functioning in conjunction with a prediction algorithm proposed by Patek et al. [35]. We evaluated the introduction of a Dynamic risk, as described in [37] to improve the algorithm performance and a more complex prediction algorithm based on an autoregressive model, presented by Sparacino et al. [38].

The reproduction of scenario 1 was useful to recreate the results of Hughes et al. [33] and test the correct simulink implementation of state of ar basal insulin modulation algorithms. The implementation of the proposed scenario 2 was necessary to create more realistic hypoglycemic episodes that could happen in real life and to have a more realistic evaluation of the algorithm performances in terms of number of hypoglycemia cases prevented and time in hypoglycemia reduction. The introduction of DR was successful in improving the performance of every modulation algorithm when compared to SR, inducing a quicker response of the insulin attenuation mechanism when observing a BG value trend approaching the hypoglycemic region. The prediction algorithms that we implemented were both efficiently able to predict the glucose trend and reduced the amount of hypoglycemic cases and time spent in hypoglycemia in every situation. Among all results, of note that by using DR plus AR with a 30 minutes PH none of the simulator virtual patients experienced severe hypoglycemia (< 55mg/dL) for more than 90 minutes, whereas the

state of art algorithm could not achieve a complete prevention. The comparison between the performances of the LP and the AR prediction algorithms suggested that no clear improvements are provided when introducing AR, even if it seems more promising when noisy data are simulated. The reason is probably the fact that the AR predictor seems to be more effective when predicting increasing BG trends rather than decreasing BG trends.
Future work will consist in:

- the creation of other different realistic physiological scenarios of hypoglycemia to test the algorithm performance, especially when the Padova/UVA simulator will be provided of new time varying insulin sensitivity modules or physical activity modules, or in presence of drugs/modifications that can alter insulin sensitivity;
- the creation of more realistic and challenging scenarios by the "technological" point of view by considering more complex/realistic CGM error modules;
- the development of new bsal insulin modulation strategies that are not exclusively based on current blood glucose value but take also into account other important variables such as the effect of the previously injected insulin boluses, e.g. by exploiting the concept of the so-called insulin on board.

Bibliography

[1] Alberti, Kurt George Matthew Mayer, and PZ ft Zimmet. "Definition, diagnosis and classification of diabetes mellitus and its complications. Part 1: diagnosis and classification of diabetes mellitus. Provisional report of a WHO consultation." Diabetic medicine 15.7 (1998): 539-553.

[2] "About diabetes". World Health Organization. Retrieved 20 february 2016. (www.who.int/diabetes/action_online/basics/en/index1.html)

[3] World Health Organization. "Definition and diagnosis of diabetes mellitus and intermediate hyperglycaemia: report of a WH." (2006).

[4] World Health Organization. "Use of glycated haemoglobin (HbA1c) in diagnosis of diabetes mellitus: abbreviated report of a WHO consultation." (2011).

[5] Morrish, N. J., et al. "Mortality and causes of death in the WHO Multinational Study of Vascular Disease in Diabetes." Diabetologia 44.2 (2001): S14-S21.

[6] Singh, Nalini, David G. Armstrong, and Benjamin A. Lipsky. "Preventing foot ulcers in patients with diabetes." Jama 293.2 (2005): 217-228.

[7] World Health Organization. Prevention of blindness from diabetes mellitus. World Health Organization, 2006.

[8] Alwan, Ala. Global status report on noncommunicable diseases 2010. World Health Organization, 2011.

[9] Roglic, Gojka, et al. "The Burden of Mortality Attributable to Diabetes Realistic estimates for the year 2000." Diabetes care 28.9 (2005): 2130-2135.

[10] http://www.diabetes.co.uk/blood-glucose/blood-glucose-self-monitoring.html

[11] Diabetes Care 2015;38(Suppl. 1):S33-S40 | DOI: 10.2337/dc15-S009

[12] Battelino, Tadej, et al. "Effect of continuous glucose monitoring on hypoglycemia in type 1 diabetes." Diabetes care 34.4 (2011): 795-800.

[13] Mauras, Nelly, et al. "Continuous glucose monitoring in type 1 diabetes."Endocrine 43.1 (2013): 41-50.

[14] http://www.dexcom.com/media/assets/dexcom-g4-platinum-mmoll

[15] Castle, Jessica R., and Peter G. Jacobs. "Nonadjunctive Use of Continuous Glucose Monitoring for Diabetes Treatment Decisions." Journal of diabetes science and technology (2016): 1932296816631569.

[16] http://www.animas.com/our-pumps/one-touch-ping

[17] http://www.diabetes.co.uk/insulin/how-insulin-pumps-work.html

[18] http://www.diabetes.co.uk/insulin-pumps/insulin-pump-dosing.html

[19] https://www.nice.org.uk/guidance/ta151

[20] Tanenberg, Robert, Christopher Newton, and I. I. I. Almond Drake. "Confirmation of hypoglycemia in the" dead-in-bed" syndrome, as captured by a retrospective continuous glucose monitoring system." Endocrine practice (2009).

[21] http://www.diabetes.co.uk/diabetic-products/pumps/lifescan-animas-vibe-insulin-pump.html

[22] Buckingham, Bruce, et al. "Preventing hypoglycemia using predictive alarm algorithms and insulin pump suspension." Diabetes technology & therapeutics 11.2 (2009): 93-97.

[23] Dassau, Eyal, et al. "Real-time hypoglycemia prediction suite using continuous glucose monitoring a safety net for the artificial pancreas."Diabetes care 33.6 (2010): 1249-1254.

[24] Oppenheim, Alan V., Ronald W. Schafer, and John R. Buck. Discrete-time signal processing. Vol. 2. Englewood Cliffs, NJ: Prentice hall, 1989.

[25] Cameron, Fraser, et al. "Statistical hypoglycemia prediction." Journal of diabetes science and technology 2.4 (2008): 612-621.

[26] Buckingham, Bruce, et al. "Prevention of nocturnal hypoglycemia using predictive alarm algorithms and insulin pump suspension." Diabetes Care33.5 (2010): 1013-1017.

[27] Palerm, Cesar C., and B. Wayne Bequette. "Hypoglycemia detection and prediction using continuous glucose monitoring, a study on hypoglycemic clamp data." Journal of diabetes science and technology 1.5 (2007): 624-629.

[28] Buckingham, Bruce A., et al. "Outpatient safety assessment of an in-home predictive low-glucose suspend system with type 1 diabetes subjects at elevated risk of nocturnal hypoglycemia." Diabetes technology & therapeutics 15.8 (2013): 622-627.

[29] Buckingham, Bruce A., et al. "Predictive low-glucose insulin suspension reduces duration of nocturnal hypoglycemia in children without increasing ketosis." Diabetes care 38.7 (2015): 1197-1204.

[30] Weiss, Ram, et al. "Predictors of hypoglycemia in the ASPIRE In-Home Study and effects of automatic suspension of insulin delivery." Journal of diabetes science and technology 9.5 (2015): 1016-1020.

[31] Agrawal, Pratik, et al. "Retrospective analysis of the real-world use of the threshold suspend feature of sensor-augmented insulin pumps." Diabetes technology & therapeutics 17.5 (2015): 316-319.

[32] Davis, T., et al. "Automated insulin pump suspension for hypoglycaemia mitigation: development, implementation and implications." Diabetes, Obesity and Metabolism 17.12 (2015): 1126-1132.

[33] Hughes, Colleen S., et al. "Hypoglycemia prevention via pump attenuation and red-yellow-green "traffic" lights using continuous glucose monitoring and insulin pump data." Journal of diabetes science and technology 4.5 (2010): 1146-1155.

[34] Bergman, Richard N., et al. "Quantitative estimation of insulin sensitivity." American Journal of Physiology-Endocrinology And Metabolism 236.6 (1979): E667.

[35] Patek, Stephen D., et al. "Modular closed-loop control of diabetes." Biomedical Engineering, IEEE Transactions on 59.11 (2012): 2986-2999.

[36] Kovatchev, Boris P., et al. "Symmetrization of the blood glucose measurement scale and its applications." Diabetes Care 20.11 (1997): 1655-1658.

[37] Guerra, Stefania, et al. "A dynamic risk measure from continuous glucose monitoring data." Diabetes technology & therapeutics 13.8 (2011): 843-852.

[38] Sparacino, Giovanni, et al. "Glucose concentration can be predicted ahead in time from continuous glucose monitoring sensor time-series." Biomedical Engineering, IEEE Transactions on 54.5 (2007): 931-937.

[39] Man, Chiara Dalla, Robert A. Rizza, and Claudio Cobelli. "Meal simulation model of the glucose-insulin system." Biomedical Engineering, IEEE Transactions on 54.10 (2007): 1740-1749.

[40] Facchinetti, Andrea, et al. "Modeling the glucose sensor error." Biomedical Engineering, IEEE Transactions on 61.3 (2014): 620-629.